NATIONAL ADVISORY COMMITTEE FOR AERONAUTICS

TECHNICAL NOTE 4188

CHARTS RELATING THE COMPRESSIVE AND SHEAR BUCKLING STRESSES OF LONGITUDINALLY SUPPORTED PLATES TO THE EFFECTIVE DEFLECTIONAL STIFFNESS OF THE SUPPORTS

By Aldie E. Johnson, Jr.

Langley Aeronautical Laboratory
Langley Field, Va.

Washington
February 1958

NATIONAL ADVISORY COMMITTEE FOR AERONAUTICS

TECHNICAL NOTE 4188

CHARTS RELATING THE COMPRESSIVE AND SHEAR BUCKLING STRESSES OF LONGITUDINALLY SUPPORTED PLATES TO THE EFFECTIVE DEFLECTIONAL STIFFNESS OF THE SUPPORTS

By Aldie E. Johnson, Jr.

SUMMARY

A stability analysis is made of long flat rectangular plates subjected to both shear and compressive loads. The edges of the plates are taken to be simply supported and the plates are supported along one or two intermediate longitudinal lines by lines of deflectional springs (elastic line supports). The results of the analysis are presented in the form of charts that are useful in the determination of the buckling load of plates stiffened by stringers or webs.

INTRODUCTION

A problem frequently encountered in the design of aircraft structures involves the determination of the shear and compressive stresses that a stiffened plate can sustain without buckling. Design information is available (refs. 1 to 3) on the stresses attainable in a stiffened plate before the onset of buckling due to either a shear or a compressive loading; but little information is available on the stresses attainable in plates subjected to combined shear and compressive loadings. Flat simply supported rectangular plates stiffened by one or more longitudinal stiffeners were analyzed in reference 1 for a shear loading and in reference 2 for a compressive loading. The present paper treats the case of combined shear and compressive loadings on long simply supported plates stiffened by one or two longitudinal stiffeners.

In the analyses of references 1 and 2, stiffeners are idealized as beam columns whose support to the plate can be expressed in terms of the area and moment of inertia of the stiffeners and the wave length of the buckles. Practical construction, however, often involves stiffening members whose support to the plate cannot be described by these parameters. Reference 3, therefore, presents a stability analysis of stiffened plates in compression in terms of a "generalized support stiffness parameter" which permits the inclusion of cross-sectional and shearing distortions of the stiffening member in an evaluation of the support offered the plate. The stability criteria of the present investigation are presented in terms of this generalized parameter. The charts given are similar to those of reference 3 and extend portions of that work to include the addition of shear loadings.

SYMBOLS

A, B	coefficients defining amplitude of support deflection
A/bt	stringer area ratio
a_n, b_n	Fourier coefficients
b	width of bay between support lines
c	ratio of average stress in stringer to average stress in plate
D	plate flexural stiffness per unit width, $\frac{Et^3}{12(1 - \mu^2)}$
E	Young's modulus of elasticity
$\frac{EI}{bD}$	bending stiffness ratio
K	coefficient
k_c	nondimensional compressive buckling-load coefficient, $\frac{N_x b^2}{\pi^2 D}$
k_s	nondimensional shear buckling-load coefficient, $\frac{N_{xy} b^2}{\pi^2 D}$
N_x	compressive load per unit width required to cause buckling
N_{xy}	shear load per unit width required to cause buckling
n	integer

Q	energy parameter
t	thickness of plate
U_1, U_2	strain energy of deformation
V_1, V_2	work of external forces
w	deflection normal to plane of plate
x, y	coordinate axes in length and width directions of plate, respectively
$\beta = \lambda/b$	
Δ_1, Δ_2, Δ_3	Lagrangian multipliers
λ	length of buckles
μ	Poisson's ratio
ψ	deflectional stiffness per unit length of support
$\psi b^3/\pi^4 D$	nondimensional deflection restraint parameter

STATEMENT OF PROBLEM

The structural configurations analyzed herein are shown in figure 1. They represent long simply supported plates which are stiffened by one or two longitudinal stringers or full-depth webs and which are subjected to shear and compressive loads. The stringers or webs (shown as springs) provide support to the plate which is simulated for the buckling mode considered herein by lines of springs with deflectional stiffness per unit length ψ. The mode of instability that is of interest is one in which the intermediate supports (lines of springs in fig. 1) deflect as the plate buckles into a series of skewed troughs and crests.

The use of lines of deflectional springs to simulate the support provided by longitudinal stringers and full-depth webs is discussed in reference 3 and utilized in references 3 to 5 to predict the behavior of aircraft structures. Reference 3 also gives the effective spring stiffness of stringers and webs in terms of the buckle length, the stress level, and geometrical properties of those members. As an example, the effective spring stiffness of a longitudinal stringer with a sturdy cross section (and hence one whose deflectional stiffness is defined by elementary beam theory) is given by the following expression:

$$\frac{\psi b^3}{\pi^4 D} = \frac{1}{\beta^4}\left(\frac{EI}{bD} - ck_C\beta^2 \frac{A}{bt}\right) \tag{1}$$

The nondimensional spring stiffness $\frac{\psi b^3}{\pi^4 D}$ in equation (1) is given in terms of nondimensional parameters commonly employed in stability analyses of stiffened plates. One of these parameters, $\frac{EI}{bD}$, is a function of the others appearing on the right-hand side of the equation. (See ref. 6.) Corresponding expressions for $\frac{\psi b^2}{\pi^4 D}$ are available in references 3 to 5 for cases in which the distortions of attachment flanges of supporting members play an important role in determining their effective spring stiffness. The reader is referred to these references for detailed discussion of this and related problems in evaluation of support stiffnesses. For simplicity, equation (1) is used in discussing applications of the results presented herein.

RESULTS

Stability criteria for the structures depicted in figure 1 are derived in the appendix by the Lagrangian multiplier method. The criterion for the two-bay structure (fig. 1(a)) is given by equation (A32) and the criterion for the three-bay structure (fig. 1(b)) is given by equation (A28). The nondimensional parameters appearing in these criteria are the buckling coefficients k_S and k_C, the buckle aspect ratio β, and the stiffness parameter $\frac{\psi b^3}{\pi^4 D}$.

The deflection functions used to derive the stability criteria are given by equations (A1) and (A29) and have symmetry about certain points (the crests and troughs of buckles) on the longitudinal center line of the plate. Solution of the stability criterion for the two-bay plate yields a single root corresponding to the first symmetric mode - a half-wave across the plate. Solution of the stability criterion for the three-bay plate yields two roots corresponding to the first two symmetric modes. However, only the results for the first symmetric mode are presented because this mode occurs at a lower stress level than the second symmetric mode and is therefore more likely to occur unless additional restraints are introduced along the support lines.

Numerical calculations were performed on the National Bureau of Standards Eastern Automatic Computer to determine the value of $\frac{\psi b^3}{\pi^4 D}$ associated with assigned values of β, k_s, and k_c. A typical set of data is given in table I. The data were reduced so that, for each configuration considered, design charts with one of the stress coefficients held constant could be constructed. The charts give, for constant values of the support stiffness, the second stress coefficient as a function of the buckle length at which buckling occurs. The charts are presented in figures 2 to 5.

Two-Bay Plate

The results of calculations on the two-bay plate are given in figures 2 and 3. Figure 2 gives values of k_s in terms of $\frac{\psi b^3}{\pi^4 D}$ and β for k_c held constant, and figure 3 gives values of k_c in terms of $\frac{\psi b^3}{\pi^4 D}$ and β for k_s held constant. Figure 3(a) ($k_s = 0$) was taken from the data of reference 3.

The results given by figure 3 of reference 1 for simply supported plates stiffened by a single longitudinal stringer can be obtained from the data of figure 2(a) ($k_c = 0$) of the present report. The value of $\frac{EI}{bD}$ given in reference 1 for a given stress level is the maximum value of $\frac{EI}{bD}$ obtained with the use of equation (1) and the combinations of $\frac{\psi b^3}{\pi^4 D}$ and β of figure 2(a) of the present report at the stress level under consideration.

Three-Bay Plate

The results of calculations on the three-bay plate are given in figures 4 and 5. Figure 4 gives values of k_s in terms of $\frac{\psi b^3}{\pi^4 D}$ and β for k_c held constant, and figure 5 gives values of k_c in terms of $\frac{\psi b^3}{\pi^4 D}$ and β for k_s held constant. Figure 5(a) was taken from the data of reference 3. As in reference 3 a cutoff to the curves is included in figure 5(a) because above this cutoff the dominant mode of instability changes from one which involves deflections of support to one in which buckling takes place with no deflection of the supports (local buckling in each bay). The curves determined by the present analysis are shown as broken lines above the cutoff in order to provide information necessary for the solution of problems in the neighborhood of the cutoff. In a manner similar to that for the two-bay plate, the data of the present report (fig. 4(a) and eq. (1)) can be used to obtain the curve for the three-bay plate given by figure 3 of reference 1.

DISCUSSION

The charts of figures 2 to 5 were designed to be applicable to plates long enough to accommodate several buckles but can be applied with reasonable accuracy to problems involving plates which buckle in as few as two or three buckles. Their use on shorter plates gives conservative results. The degree of conservatism may be large or small depending upon the problem under consideration. In the case of rectangular plates subjected to compressive loads, the plate is terminated by ribs which contact the plate on a line that is also a natural nodal line of the buckled plate, and the results obtained from the charts are exact. Plates stiffened by sturdy longitudinal stringers and chordwise ribs usually develop buckles whose length is large in comparison with the width of the plate as will be demonstrated later. The rib spacing for these structures may be such that the plate buckles into a single half-wave between ribs, and use of the charts will give conservative results except in the case of a pure compressive loading. Plates stiffened by stringers or webs which do not behave as sturdy stringers often develop buckles whose length is of the order of the plate width. The charts can be used for these structures with good results because ribs are usually several plate widths apart. The degree of conservatism may be large, however, for plates with small rib spacings which are subjected to shear stresses. For instance, as an extreme example, if the shear buckling coefficient for a simply supported square plate is obtained from the charts presented herein $\left(\text{from fig. 2(a) with } \beta = 2 \text{ and } \frac{\psi b^3}{\pi^4 D} = 0 \text{ or from fig. 4(a) with } \beta = 3 \text{ and } \frac{\psi b^3}{\pi^4 D} = 0\right)$, a value of 5.5 is obtained after the values of k_s read from figures 2(a) and 4(a) are multiplied by 2^2 and 3^2, respectively, to convert them to buckling coefficients in which the plate width b is the distance between the simply supported edges. The correct value for this case is 9.3. The difference between these two numbers reflects the effect of restraint on the buckle shape near the ends of the plate.

An application of the charts presented herein is given in figures 6 and 7 where interaction curves for two-bay and three-bay plates stiffened by sturdy longitudinal stringers of particular proportions are presented. The curves were drawn with the use of figures 2 to 5 and equation (1). The discontinuities in the interaction curves result from a change in the mode of instability analogous to the change in mode responsible for the cutoff in figure 5(a). The upper section of a given curve $\left(\text{curve for constant } \frac{EI}{bD}\right)$ corresponds to a mode of instability in which the supports deflect with the plate. The lower section (from ref. 7) corresponds to a mode of instability in which buckling takes place without deflection of the supports. Thus, from such curves, the mode of instability and the combination of shear and compressive stresses that can be carried by an infinitely long longitudinally stiffened plate can be determined directly.

Another application of the design charts presented herein is given in figure 8 where the data of figure 2(a) are presented in an alternate form which illustrates the behavior of plates stiffened by sturdy longitudinal stringers. The results shown for the particular case of a two-bay plate loaded in shear are qualitatively similar to those for plates with two or more bays loaded in compression or in compression and shear. When the bending stiffness of the longitudinal stringer is zero (that is, the stringer is inactive or nonexistent), the plate buckles as a simply supported plate at $k_s = 1.33$ and $\beta = 2.4$. The corresponding critical stress and buckle length check those found in other investigations (ref. 8, for example). As the bending stiffness of the stringer is increased, the critical stress and wave length increase. Finally, in this process a value of $\frac{EI}{bD}$ can be found ($\approx$1,750) so that the plate may buckle into either of two modes with values of β that differ by a factor of about 10 for the particular case considered. For larger values of $\frac{EI}{bD}$, the plate buckles at the shorter wave length at values of k_s which approximate those computed for a plate simply supported at the stringer. In the comparable problem for a two-bay plate loaded in compression, the buckling coefficient for the deflection function used approximates that of a plate clamped at the stringer when the bending stiffness of the stringer is large so that the plate buckles at the shorter wave lengths.

Further applications of charts like those presented herein are presented in considerable detail in reference 3.

CONCLUDING REMARKS

Design charts have been presented which evaluate the combination of shear and compressive stresses required to buckle long flat simply supported rectangular plates stiffened by one or two intermediate lines of deflectional springs (elastic line supports). The charts are applicable to the determination of the buckling load of plates stiffened by stringers or webs of proportions encountered in aircraft construction.

Langley Aeronautical Laboratory,
National Advisory Committee for Aeronautics,
Langley Field, Va., September 30, 1957.

APPENDIX

DERIVATION OF STABILITY CRITERIA

Stability criteria are derived by means of the Lagrangian multiplier method for the buckling under combined axial compression and shear of the simply supported plate configurations shown in figure 1.

Three-Bay Plate

The deflection function used to represent the buckled shape of the plate of figure 1(b) is given by the series

$$w = \sin\frac{\pi x}{\lambda}\sum_{n=1,3,5,\ldots}^{\infty} a_n \sin\frac{n\pi y}{3b} + \cos\frac{\pi x}{\lambda}\sum_{n=1,3,5,\ldots}^{\infty} b_n \cos\frac{n\pi y}{3b} \qquad \text{(A1)}$$

with the origin of the coordinates as shown in figure 1. This deflection function can provide the desired buckle shape, but the required geometric boundary conditions of zero deflection at the edges are not satisfied term by term. The required conditions, which can be written

$$w(x,0) = w(x,3b) = 0 \qquad \text{(A2)}$$

will be introduced by means of Lagrangian multipliers.

The deflection of the first line of deflectional springs w_b can be represented by

$$w_b = A \sin\frac{\pi x}{\lambda} + B \cos\frac{\pi x}{\lambda} \qquad \text{(A3)}$$

From symmetry considerations, the deflection of the second line of deflectional springs w_{2b} can be represented by

$$w_{2b} = A \sin\frac{\pi x}{\lambda} - B \cos\frac{\pi x}{\lambda} \qquad \text{(A4)}$$

The condition that the deflection of the springs is equal to the deflection of the plate along the attachment lines

$$w_b(x) = w(x,b) \tag{A5}$$

$$w_{2b}(x) = w(x,2b) \tag{A6}$$

will also be introduced by means of Lagrangian multipliers.

The internal energy of the plate-support system is the sum of the strain energy of bending of the plate and the energy of the deflectional springs. The strain energy of a plate of stiffness D is

$$U_1 = \frac{D}{2}\int_0^{\lambda}\int_0^{3b}\left\{\left(\frac{\partial^2 w}{\partial x^2} + \frac{\partial^2 w}{\partial y^2}\right)^2 - 2(1 - \mu)\left[\frac{\partial^2 w}{\partial x^2}\frac{\partial^2 w}{\partial y^2} - \left(\frac{\partial^2 w}{\partial x\,\partial y}\right)^2\right]\right\}dx\,dy$$

$$= \frac{3\pi^4 bD}{8\lambda^3}\left\{\sum_{n=1,3,5,\ldots}^{\infty} a_n^2\left(1 + \frac{n^2\lambda^2}{9b^2}\right) + \sum_{n=1,3,5,\ldots}^{\infty}\left[b_n\left(1 + \frac{n^2\lambda^2}{9b^2}\right) - \frac{\lambda^2 K}{9b^2}\right]^2\right\} \tag{A7}$$

where K is an undetermined coefficient that arises from the "exact" differentiation of the series. The energy of the deflectional springs which have a spring constant ψ is

$$U_2 = \frac{\psi}{2}\int_0^{\lambda} w_b^2 dx + \frac{\psi}{2}\int_0^{\lambda} w_{2b}^2 dx = \frac{4\lambda^4}{3\pi^4 bD}\,\frac{3\pi^4 bD}{8\lambda^3}\,\psi\left(A^2 + B^2\right) \tag{A8}$$

The external work is in two parts. The work done by the shearing forces N_{xy} is

$$V_1 = -N_{xy}\int_0^{\lambda}\int_0^{3b}\left(\frac{\partial w}{\partial x}\frac{\partial w}{\partial y}\right)dx\,dy = \frac{\pi^2}{2}N_{xy}\sum_{n=1,3,5,\ldots}^{\infty} a_n b_n n \tag{A9}$$

The work done by the uniform compressive forces N_x is

$$V_2 = N_x \int_0^{\lambda} \int_0^{3b} \left(\frac{\partial w}{\partial x}\right)^2 dx\, dy = \frac{N_x}{2}\left(\frac{3\pi^2 b}{4\lambda}\right)\left(\sum_{n=1,3,5,\ldots}^{\infty} a_n^2 + \sum_{n=1,3,5,\ldots}^{\infty} b_n^2\right) \tag{A10}$$

Then

$$\begin{aligned}\frac{8\lambda^3}{3\pi^4 Db}\left(U_1 + U_2 - V_1 - V_2\right) = &\sum_{n=1,3,5,\ldots}^{\infty} a_n^2\left(1 + \frac{n^2\beta^2}{9}\right)^2 + \\ &\sum_{n=1,3,5,\ldots}^{\infty}\left[b_n\left(1 + \frac{n^2\beta^2}{9}\right)^2 - \frac{\beta^2 K}{9}\right]^2 + \\ &\frac{4\beta^4}{3}\frac{\psi b^3}{\pi^4 D}\left(A^2 + B^2\right) - \frac{4\beta^3}{3}k_s\left(\sum_{n=1,3,5,\ldots}^{\infty} a_n b_n n\right) - \\ &\beta^2 k_c\left(\sum_{n=1,3,5,\ldots}^{\infty} a_n^2 + \sum_{n=1,3,5,\ldots}^{\infty} b_n^2\right)\end{aligned} \tag{A11}$$

where

$$\beta = \frac{\lambda}{b} \qquad k_s = \frac{N_{xy} b^2}{\pi^2 D} \qquad k_c = \frac{N_x b^2}{\pi^2 D}$$

and $\frac{\psi b^3}{\pi^4 D}$ is a nondimensional deflectional spring stiffness parameter.

In order to satisfy the boundary condition of zero deflection (eq. (A2)) and the condition that the deflection of the springs equals the deflection of the plate (eqs. (A5) and (A6)), it is necessary to impose the following constraint relationships:

$$\sum_{n=1,3,5,\ldots}^{\infty} b_n = 0 \tag{A12}$$

$$\sum_{n=1,3,5,\ldots}^{\infty} a_n \sin\frac{n\pi}{3} - A = 0 \tag{A13}$$

$$\sum_{n=1,3,5,\ldots}^{\infty} b_n \cos\frac{n\pi}{3} - B = 0 \tag{A14}$$

According to the Lagrangian multiplier method, the expression to be minimized is

$$Q = \frac{8\lambda^3}{3\pi^4 bD}\left(U_1 + U_2 - V_1 - V_2\right) - \Delta_1\left(\sum_{n=1,3,5,\ldots}^{\infty} a_n \sin\frac{n\pi}{3} - A\right) -$$

$$\Delta_2\left(\sum_{n=1,3,5,\ldots}^{\infty} b_n \cos\frac{n\pi}{3} - B\right) - \Delta_3\left(\sum_{n=1,3,5,\ldots}^{\infty} b_n\right) \tag{A15}$$

where Δ_1, Δ_2, and Δ_3 are the Lagrangian multipliers.

The expressions for Q must be minimized with respect to a_n, b_n, K, A, B, Δ_1, Δ_2, and Δ_3. Minimization yields the following equations:

$$\frac{\partial Q}{\partial a_n} = a_n\left[\left(\frac{1 + n^2\beta^2}{9}\right)^2 - \beta^2 k_C\right] - \frac{\beta^3 k_S n b_n}{3} + \Delta_1 \sin\frac{n\pi}{3} = 0$$

$$(n = 1, 3, 5, \ldots \infty) \tag{A16}$$

$$\frac{\partial Q}{\partial b_n} = b_n\left[\left(1 + \frac{n^2\beta^2}{9}\right)^2 - \beta^2 k_C\right] - \frac{\left(1 + \frac{n^2\beta^2}{9}\right)\beta^2 K}{9} - \frac{2\beta^3 k_S a_n n}{3} +$$

$$\Delta_2 \cos\frac{n\pi}{3} + \Delta_3 = 0 \qquad (n = 1, 3, 5, \ldots \infty) \tag{A17}$$

$$\frac{\partial Q}{\partial K} = -\sum_{n=1,3,5,\ldots}^{\infty} \frac{b_n\left(1 + \frac{n^2\beta^2}{9}\right)\beta^2}{9} + \frac{\beta^4}{81} K = 0 \tag{A18}$$

$$\frac{\partial Q}{\partial A} = \frac{4\beta^4 A}{3} \frac{\psi b^3}{\pi^4 D} - \Delta_1 = 0 \tag{A19}$$

$$\frac{\partial Q}{\partial B} = \frac{4\beta^4 B}{3} \frac{\psi b^3}{\pi^4 D} - \Delta_2 = 0 \tag{A20}$$

$$\frac{\partial Q}{\partial \Delta_1} = \sum_{n=1,3,5,\ldots}^{\infty} a_n \sin\frac{n\pi}{3} - A = 0 \tag{A21}$$

$$\frac{\partial Q}{\partial \Delta_2} = \sum_{n=1,3,5,\ldots}^{\infty} b_n \cos\frac{n\pi}{3} - B = 0 \tag{A22}$$

$$\frac{\partial Q}{\partial \Delta_3} = \sum_{n=1,3,5,\ldots}^{\infty} b_n = 0 \tag{A23}$$

Equations (A16), (A17), (A19), and (A20) may be solved for a_n, b_n, A, and B, respectively, and the resulting expressions substituted into equations (A18), (A21), (A22), and (A23). This substitution results in the following set of simultaneous homogeneous equations:

$$\frac{K\beta^2}{9}\left[\sum_{n=1,3,5,\ldots}^{\infty}\left(\frac{A_n{}^2 B_n}{B_n{}^2 - C_n{}^2} - 1\right)\right] - \Delta_1\left(\sum_{n=1,3,5,\ldots}^{\infty}\frac{A_n C_n \sin\frac{n\pi}{3}}{B_n{}^2 - C_n{}^2}\right) -$$

$$\Delta_2\left(\sum_{n=1,3,5,\ldots}^{\infty}\frac{A_n B_n \cos\frac{n\pi}{3}}{B_n{}^2 - C_n{}^2}\right) - \Delta_3\left(\sum_{n=1,3,5,\ldots}^{\infty}\frac{A_n B_n}{B_n{}^2 - C_n{}^2}\right) = 0 \tag{A24}$$

$$\frac{K\beta^2}{9}\left(\sum_{n=1,3,5,\ldots}^{\infty} \frac{A_nC_n \sin\frac{n\pi}{3}}{B_n{}^2 - C_n{}^2}\right) - \Delta_1\left(\frac{1}{\frac{4\beta^4}{3}\frac{\psi b^3}{\pi^4 D}} + \sum_{n=1,3,5,\ldots}^{\infty} \frac{B_n \sin^2\frac{n\pi}{3}}{B_n{}^2 - C_n{}^2}\right) -$$

$$\Delta_2\left(\sum_{n=1,3,5,\ldots}^{\infty} \frac{C_n \cos\frac{n\pi}{3}\sin\frac{n\pi}{3}}{B_n{}^2 - C_n{}^2}\right) - \Delta_3\left(\sum_{n=1,3,5,\ldots}^{\infty} \frac{C_n \sin\frac{n\pi}{3}}{B_n{}^2 - C_n{}^2}\right) = 0 \qquad \text{(A25)}$$

$$\frac{K\beta^2}{9}\left(\sum_{n=1,3,5,\ldots}^{\infty} \frac{A_nB_n \cos\frac{n\pi}{3}}{B_n{}^2 - C_n{}^2}\right) - \Delta_1\left(\sum_{n=1,3,5,\ldots}^{\infty} \frac{C_n \sin\frac{n\pi}{3}\cos\frac{n\pi}{3}}{B_n{}^2 - C_n{}^2}\right) -$$

$$\Delta_2\left(\sum_{n=1,3,5,\ldots}^{\infty} \frac{B_n \cos^3\frac{n\pi}{3}}{B_n{}^2 - C_n{}^2} + \frac{1}{\frac{4\beta^4}{3}\frac{\psi b^3}{\pi^4 D}}\right) - \Delta_3\left(\sum_{n=1,3,5,\ldots}^{\infty} \frac{B_n \cos\frac{n\pi}{3}}{B_n{}^2 - C_n{}^2}\right) = 0 \qquad \text{(A26)}$$

$$\frac{K\beta^2}{9}\left(\sum_{n=1,3,5,\ldots}^{\infty} \frac{A_nB_n}{B_n{}^2 - C_n{}^2}\right) - \Delta_1\left(\sum_{n=1,3,5,\ldots}^{\infty} \frac{C_n \sin\frac{n\pi}{3}}{B_n{}^2 - C_n{}^2}\right) -$$

$$\Delta_2\left(\sum_{n=1,3,5,\ldots}^{\infty} \frac{B_n \cos\frac{n\pi}{3}}{B_n{}^2 - C_n{}^2}\right) - \Delta_3\left(\sum_{n=1,3,5,\ldots}^{\infty} \frac{B_n}{B_n{}^2 - C_n{}^2}\right) = 0 \qquad \text{(A27)}$$

where

$$A_n = 1 + \frac{n^2\beta^2}{9}$$

$$B_n = \left(1 + \frac{n^2\beta^2}{9}\right)^2 - \beta^2 k_C$$

$$C_n = \frac{2}{3}\beta^3 n k_S$$

Equations (A24) to (A27), when combined into determinantal form, yield the following stability criterion:

$$\begin{vmatrix} \sum\limits_{n=1,3,5,\ldots}^{\infty}\left\{\frac{\left(1+\frac{\beta^2n^2}{9}\right)^2\left[\left(1+\frac{\beta^2n^2}{9}\right)^2-\beta^2k_c\right]}{E_n}-1\right\} & \sum\limits_{n=1,3,5,\ldots}^{\infty}\frac{\left(1+\frac{\beta^2n^2}{9}\right)\left[\left(1+\frac{\beta^2n^2}{9}\right)^2-\beta^2k_c\right]}{E_n} & \sum\limits_{n=1,3,5,\ldots}^{\infty}\frac{\left(1+\frac{\beta^2n^2}{9}\right)\left(\frac{2}{3}\beta^3nk_s\right)\sin\frac{n\pi}{2}}{E_n} & \sum\limits_{n=1,3,5,\ldots}^{\infty}\frac{\left(1+\frac{\beta^2n^2}{9}\right)\left[\left(1+\frac{\beta^2n^2}{9}\right)^2-\beta^2k_c\right]\cos\frac{n\pi}{2}}{E_n} \\ \sum\limits_{n=1,3,5,\ldots}^{\infty}\frac{\left(1+\frac{\beta^2n^2}{9}\right)\left[\left(1+\frac{\beta^2n^2}{9}\right)^2-\beta^2k_c\right]}{E_n} & \sum\limits_{n=1,3,5,\ldots}^{\infty}\frac{\left(1+\frac{\beta^2n^2}{9}\right)^2-\beta^2k_c}{E_n} & \sum\limits_{n=1,3,5,\ldots}^{\infty}\frac{\left(\frac{2}{3}\beta^3nk_s\right)\sin\frac{n\pi}{2}}{E_n} & \sum\limits_{n=1,3,5,\ldots}^{\infty}\frac{\left[\left(1+\frac{\beta^2n^2}{9}\right)^2-\beta^2k_c\right]\cos\frac{n\pi}{2}}{E_n} \\ \sum\limits_{n=1,3,5,\ldots}^{\infty}\frac{\left(1+\frac{\beta^2n^2}{9}\right)\left(\frac{2}{3}\beta^3nk_s\right)\sin\frac{n\pi}{2}}{E_n} & \sum\limits_{n=1,3,5,\ldots}^{\infty}\frac{\left(\frac{2}{3}\beta^3nk_s\right)\sin\frac{n\pi}{2}}{E_n} & \sum\limits_{n=1,3,5,\ldots}^{\infty}\left\{\frac{\left[\left(1+\frac{\beta^2n^2}{9}\right)^2-\beta^2k_c\right]\sin^2\frac{n\pi}{2}}{E_n}+\frac{3}{\beta^4\frac{EI}{bD}}\right\} & \sum\limits_{n=1,3,5,\ldots}^{\infty}\frac{\left(\frac{2}{3}\beta^3nk_s\right)\sin\frac{n\pi}{2}\cos\frac{n\pi}{2}}{E_n} \\ \sum\limits_{n=1,3,5,\ldots}^{\infty}\frac{\left(1+\frac{\beta^2n^2}{9}\right)\left[\left(1+\frac{\beta^2n^2}{9}\right)^2-\beta^2k_c\right]\cos\frac{n\pi}{2}}{E_n} & \sum\limits_{n=1,3,5,\ldots}^{\infty}\frac{\left[\left(1+\frac{\beta^2n^2}{9}\right)^2-\beta^2k_c\right]\cos\frac{n\pi}{2}}{E_n} & \sum\limits_{n=1,3,5,\ldots}^{\infty}\frac{\left(\frac{2}{3}\beta^3nk_s\right)\sin\frac{n\pi}{2}\cos\frac{n\pi}{2}}{E_n} & \sum\limits_{n=1,3,5,\ldots}^{\infty}\left\{\frac{\left[\left(1+\frac{\beta^2n^2}{9}\right)^2-\beta^2k_c\right]\cos^2\frac{n\pi}{2}}{E_n}+\frac{3}{\beta^4\frac{EI}{bD}}\right\} \end{vmatrix} = 0 \tag{A28}$$

where

$$E_n = \left[\left(1 + \frac{\beta^2n^2}{9}\right)^2 - \beta^2k_c\right]^2 - \left(\frac{2}{3}\beta^3nk_s\right)^2$$

Two-Bay Plate

The following deflection function is used to represent the buckled shape of the plate of figure 1(a):

$$w = \sin\frac{\pi x}{\lambda}\sum_{n=1,3,5,\ldots}^{\infty} a_n \sin\frac{n\pi y}{2b} + \cos\frac{\pi x}{\lambda}\sum_{n=1,3,5,\ldots}^{\infty} b_n \cos\frac{n\pi y}{2b} \tag{A29}$$

Lagrangian multipliers are used to introduce the conditions of zero deflection at the edges of the plate and the condition of compatibility of deflection of plate and springs along the attachment line. These conditions are

$$w(x,0) = w(x,2b) = 0 \tag{A30}$$

$$w_b(x) = w(x,b) \tag{A31}$$

The internal energies and external work are computed in the same way as for the three-bay plate and are minimized with respect to the same coefficients. The stability criterion thus determined is

$$\begin{vmatrix} \sum_{n=1,3,5,\ldots}^{\infty}\left\{\frac{\left(1+\frac{\beta^2n^2}{4}\right)^2\left[\left(1+\frac{\beta^2n^2}{4}\right)^2-\beta^2k_c\right]}{D_n}-1\right\} & \sum_{n=1,3,5,\ldots}^{\infty}\frac{\left(1+\frac{\beta^2n^2}{4}\right)\left[\left(1+\frac{\beta^2n^2}{4}\right)^2-\beta^2k_c\right]}{D_n} & \sum_{n=1,3,5,\ldots}^{\infty}\frac{\left(1+\frac{\beta^2n^2}{4}\right)\beta^3nk_s\sin\frac{n\pi}{2}}{D_n} \\ \sum_{n=1,3,5,\ldots}^{\infty}\frac{\left(1+\frac{\beta^2n^2}{4}\right)\left[\left(1+\frac{\beta^2n^2}{4}\right)^2-\beta^2k_c\right]}{D_n} & \sum_{n=1,3,5,\ldots}^{\infty}\frac{\left(1+\frac{\beta^2n^2}{4}\right)^2-\beta^2k_c}{D_n} & \sum_{n=1,3,5,\ldots}^{\infty}\frac{\beta^3nk_s\sin\frac{n\pi}{2}}{D_n} \\ \sum_{n=1,3,5,\ldots}^{\infty}\frac{\left(1+\frac{\beta^2n^2}{4}\right)\beta^3nk_s\sin\frac{n\pi}{2}}{D_n} & \sum_{n=1,3,5,\ldots}^{\infty}\frac{\beta^3nk_s\sin\frac{n\pi}{2}}{D_n} & \sum_{n=1,3,5,\ldots}^{\infty}\left\{\frac{\left[\left(1+\frac{\beta^2n^2}{4}\right)^2-\beta^2k_c\right]\sin^2\frac{n\pi}{2}}{D_n}+\frac{1}{\beta^4\frac{kb^3}{\pi^4D}}\right\} \end{vmatrix} = 0 \tag{A32}$$

where

$$D_n = \left[\left(1+\frac{\beta^2n^2}{4}\right)^2-\beta^2k_c\right]^2-\left(\beta^3nk_s\right)^2$$

REFERENCES

1. Crate, Harold, and Lo, Hsu: Effect of Longitudinal Stiffeners on the Buckling Load of Long Flat Plates Under Shear. NACA TN 1589, 1948.

2. Seide, Paul, and Stein, Manuel: Compressive Buckling of Simply Supported Plates With Longitudinal Stiffeners. NACA TN 1825, 1949.

3. Anderson, Roger A., and Semonian, Joseph W.: Charts Relating the Compressive Buckling Stress of Longitudinally Supported Plates to the Effective Deflectional and Rotational Stiffness of the Supports. NACA Rep. 1202, 1954. (Supersedes NACA TN 2987.)

4. Semonian, Joseph W., and Anderson, Roger A.: An Analysis of the Stability and Ultimate Bending Strength of Multiweb Beams With Formed-Channel Webs. NACA TN 3232, 1954.

5. Semonian, Joseph W., and Peterson, James P.: An Analysis of the Stability and Ultimate Compressive Strength of Short Sheet-Stringer Panels With Special Reference to the Influence of the Riveted Connection Between Sheet and Stringer. NACA Rep. 1255, 1956. (Supersedes NACA TN 3431.)

6. Seide, Paul: The Effect of Longitudinal Stiffeners Located on One Side of a Plate on the Compressive Buckling Stress of the Plate-Stiffener Combination. NACA TN 2873, 1953.

7. Stowell, Elbridge Z., and Schwartz, Edward B.: Critical Stress for an Infinitely Long Flat Plate With Elastically Restrained Edges Under Combined Shear and Direct Stress. NACA WR L-340, 1943. (Formerly NACA ARR 3K13.)

8. Stowell, Elbridge Z.: Critical Shear Stress of an Infinitely Long Flat Plate With Equal Elastic Restraints Against Rotation Along the Parallel Edges. NACA WR L-476, 1943. (Formerly NACA ARR 3K12.)

TABLE I.- VALUES OF DEFLECTIONAL STIFFNESS PARAMETER $\frac{\psi b^3}{\pi^4 D}$ FOR TWO-BAY PLATE

$[k_c = 3.0]$

k_s	$\frac{\psi b^3}{\pi^4 D}$ for values of β of -											
	0.6	0.8	1.0	1.2	1.5	2.0	3.0	3.5	4.0	5.0	6.0	7.0
0	-0.781	1.713	1.877	1.527	1.029	0.561	0.213	0.139	0.0917	0.0362	0.00618	-0.0119
.10	--------	-------	-------	------	--------	-------	------	-----	------	------	.00639	--------
.50	-.693	1.855	2.035	------	1.123	.613	.234	.155	.104	.0457	.0114	-.00806
.75	--------	-------	-------	------	--------	.679	------	-----	------	------	-------	--------
1.00	-.422	2.311	2.554	2.115	1.427	.776	.301	.203	.140	.0665	.0270	.00338
1.25	--------	-------	-------	------	--------	.902	------	-----	------	------	-------	--------
1.50	--------	-------	-------	------	--------	1.066	.415	.284	.201	.105	.0533	.0226
2.00	.786	4.753	6.053	5.169	3.132	1.537	.584	.403	.289	.159	.0906	.0496
2.50	--------	7.987	17.72	14.29	5.607	2.285	.817	.563	.407	.231	.139	.0849
2.60	--------	-------	32.51	------	--------	-------	------	-----	------	------	-------	--------
2.70	--------	-------	-------	65.51	--------	-------	------	-----	------	------	-------	--------
2.75	--------	-------	-60.85	------	--------	-------	------	-----	------	------	-------	--------
3.00	3.429	22.21	-5.704	------	17.48	3.563	1.132	.773	.558	.322	.200	.129
3.10	--------	-------	-------	------	30.37	-------	------	-----	------	------	-------	--------
3.20	--------	-------	-------	------	129.4	-------	------	-----	------	------	-------	--------
3.26	--------	-66.18	-------	------	-185.2	-------	------	-----	------	------	-------	--------
3.50	--------	-3.246	-------	------	--------	6.212	1.557	1.044	.749	.433	.274	.181
4.00	10.12	11.95	12.42	------	-1.968	16.08	2.141	-----	.986	------	.361	--------
4.10	--------	-------	-------	------	-1.084	-------	------	-----	------	------	-------	--------
4.25	--------	-------	-------	------	--------	65.07	------	-----	------	------	-------	--------
4.50	20.83	46.74	-------	------	--------	-29.82	------	-----	------	------	-------	--------
4.75	43.75	-------	-------	------	--------	-------	------	-----	------	------	-------	--------
5.00	-42.14	-93.46	-86.00	------	6.426	-6.113	4.260	-----	1.654	------	.583	--------
5.10	--------	-------	-------	------	--------	-4.918	------	-----	------	------	-------	--------
6.00	-682.5	-18.76	-17.25	------	63.67	1.225	11.87	-----	2.750	------	.882	--------

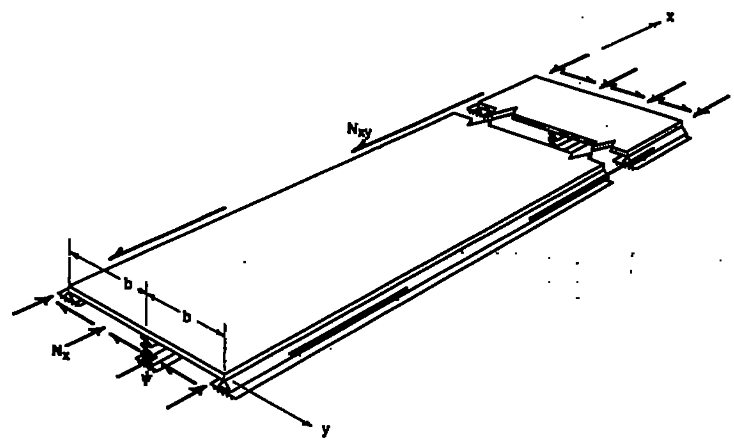

(a) One line of support.

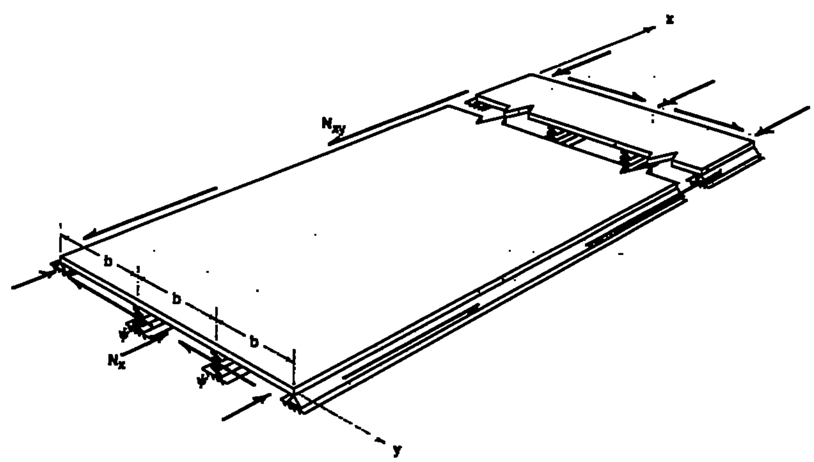

(b) Two lines of support.

Figure 1.- Structural configuration and loading investigated.

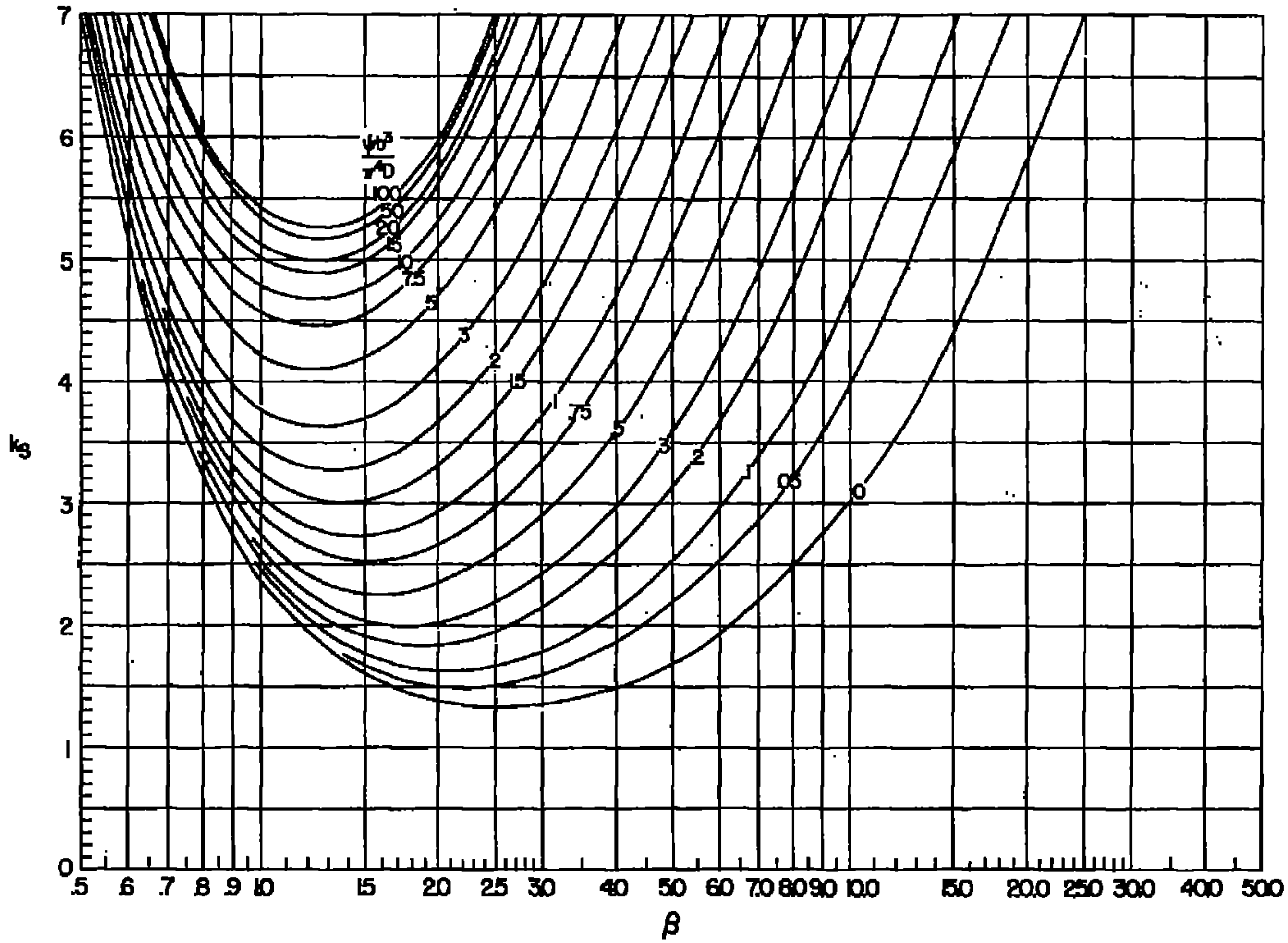

(a) $k_C = 0$.

Figure 2.- Stability curves for two-bay plate with constant compressive load.

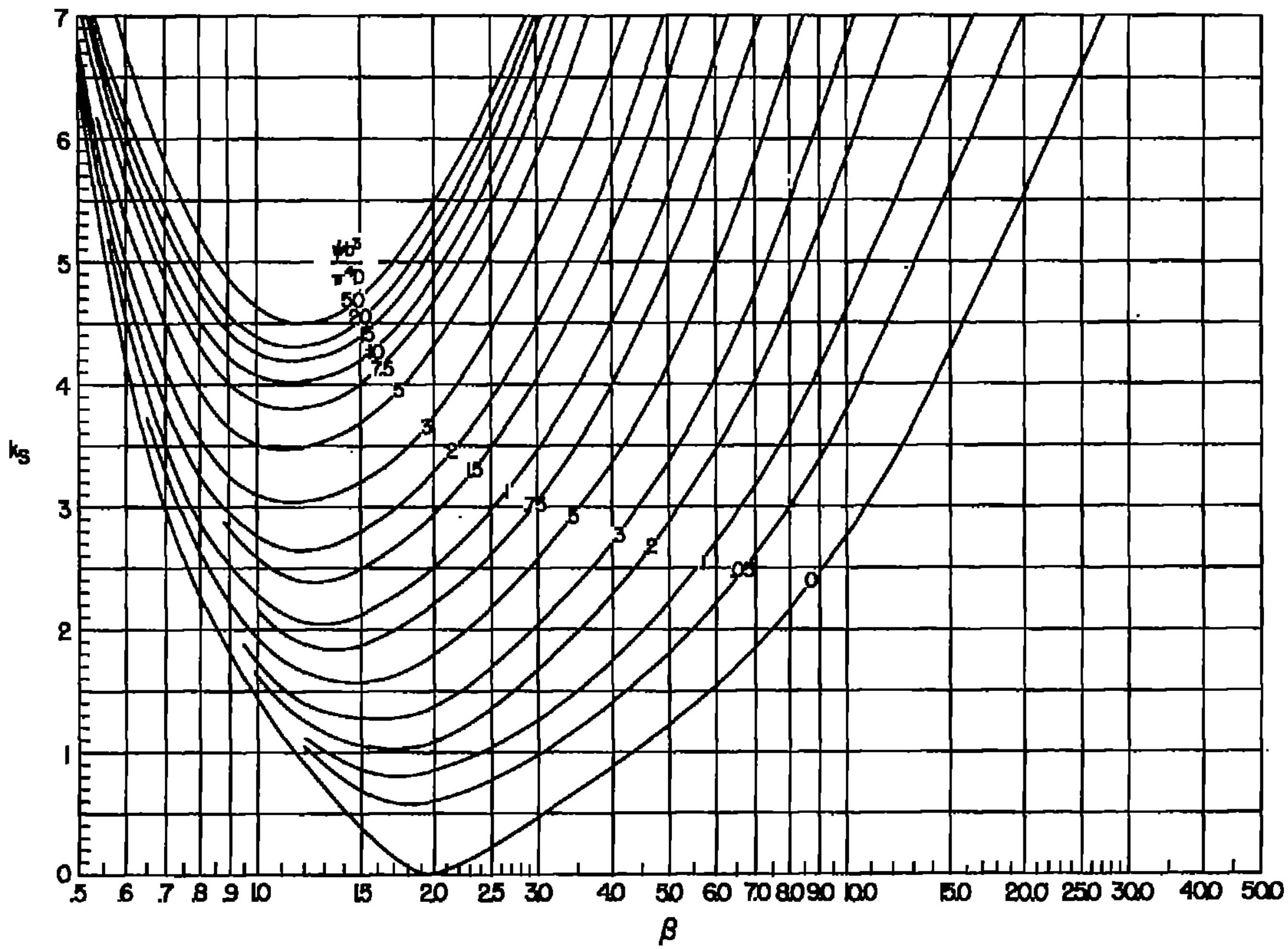

(b) $k_C = 1$.

Figure 2.- Continued.

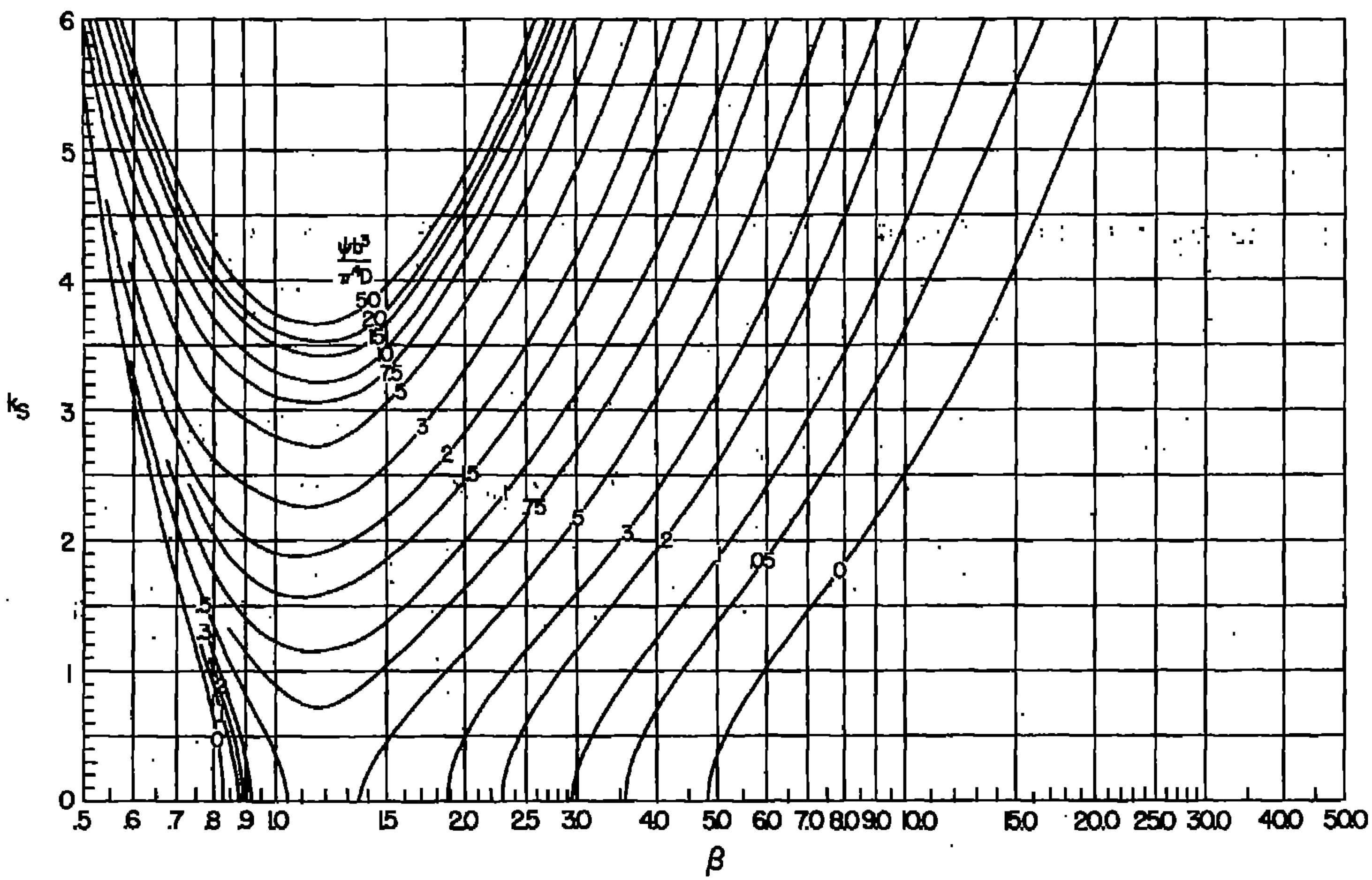

(c) $k_C = 2$.

Figure 2.- Continued.

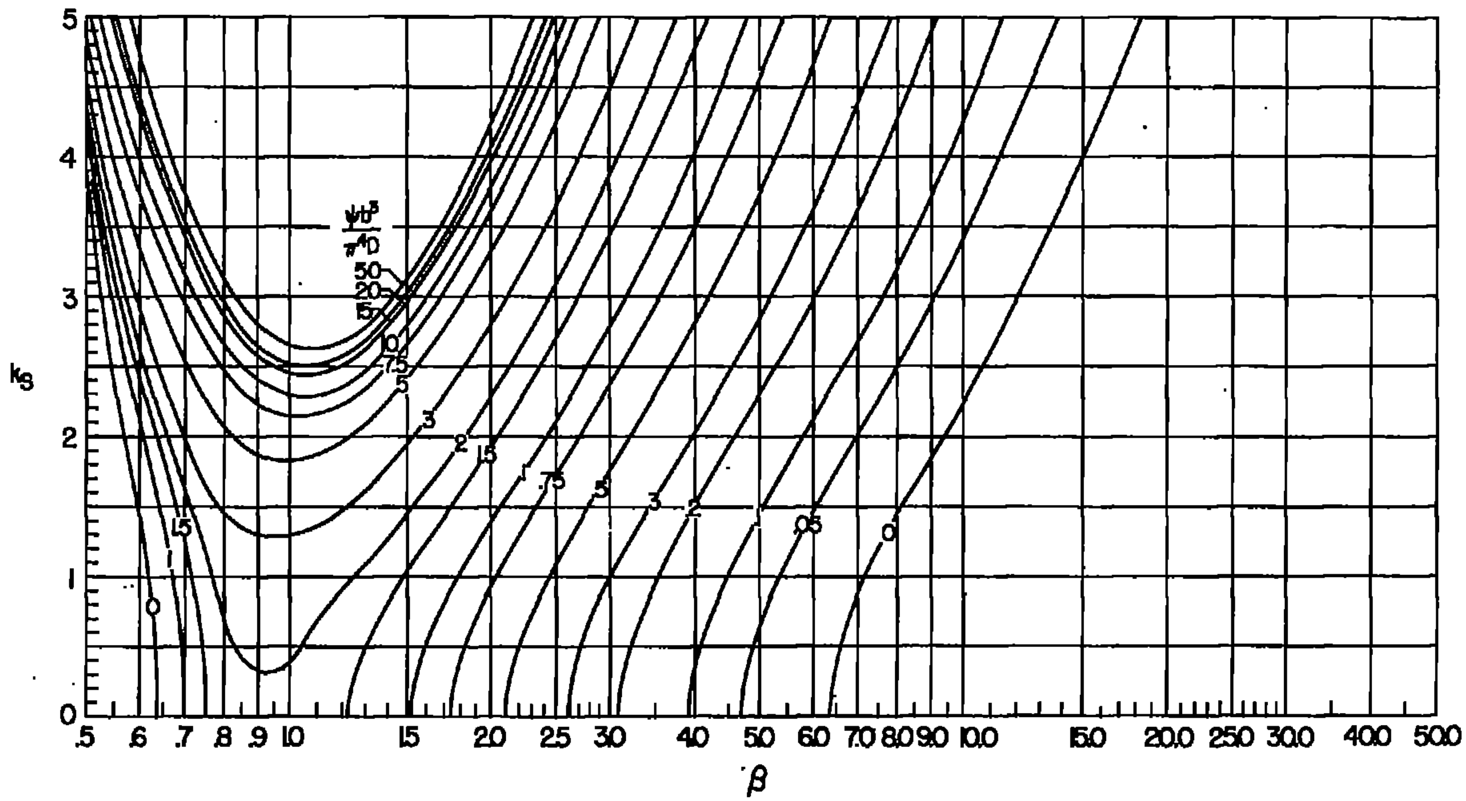

(d) $k_c = 3$.

Figure 2.- Continued.

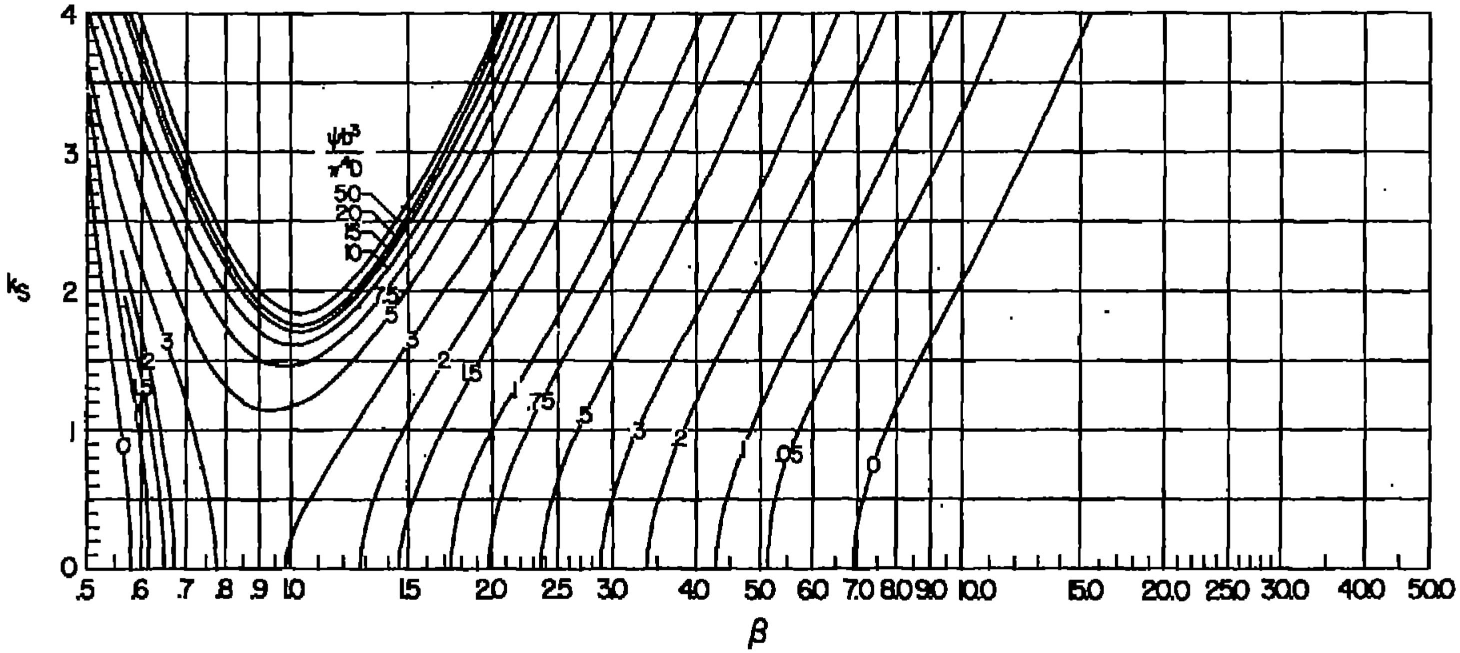

(e) $k_C = 3.5$.

Figure 2.- Concluded.

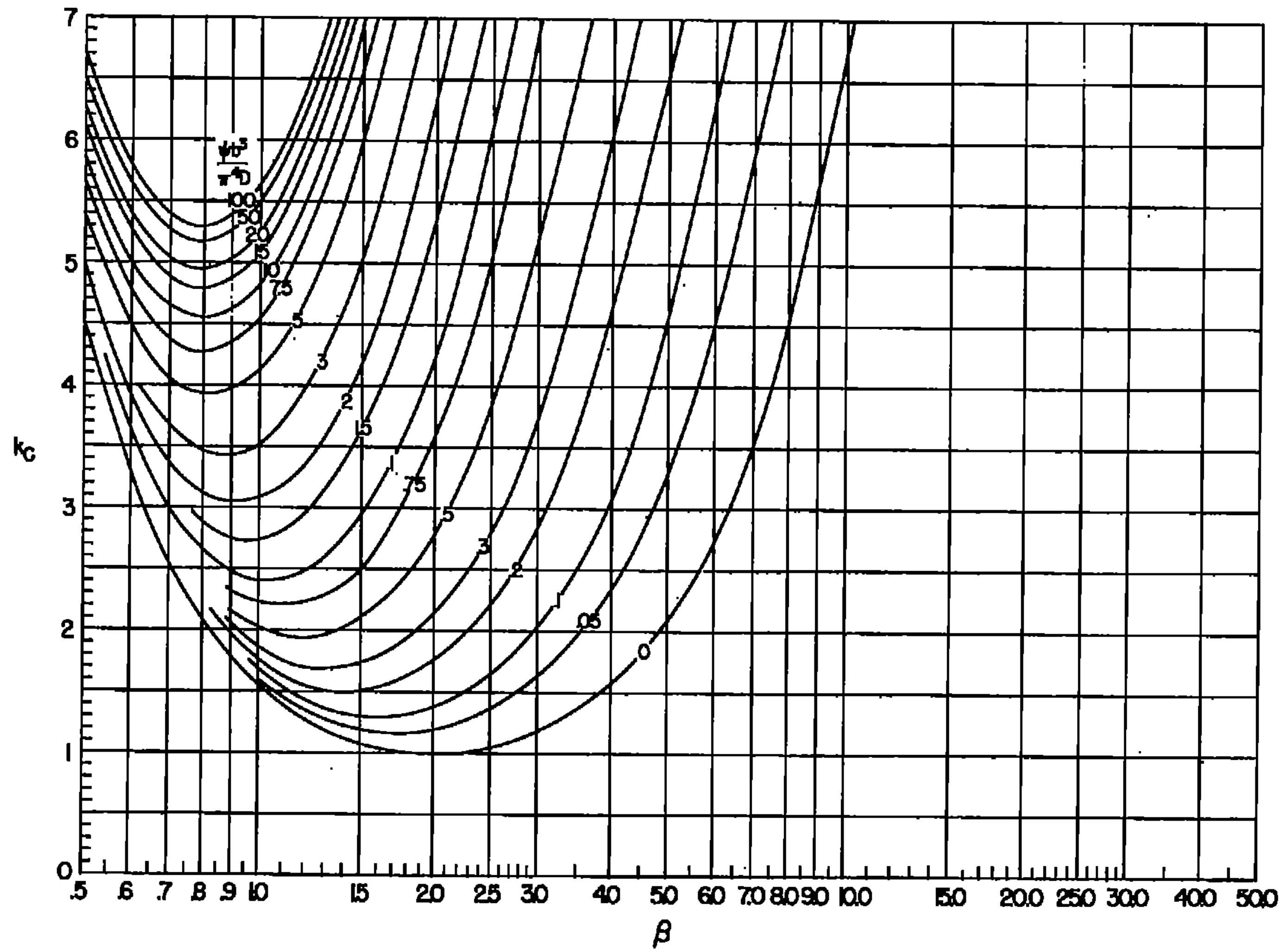

(a) $k_s = 0$. (Data are from ref. 3.)

Figure 3.- Stability curves for two-bay plate with constant shear load.

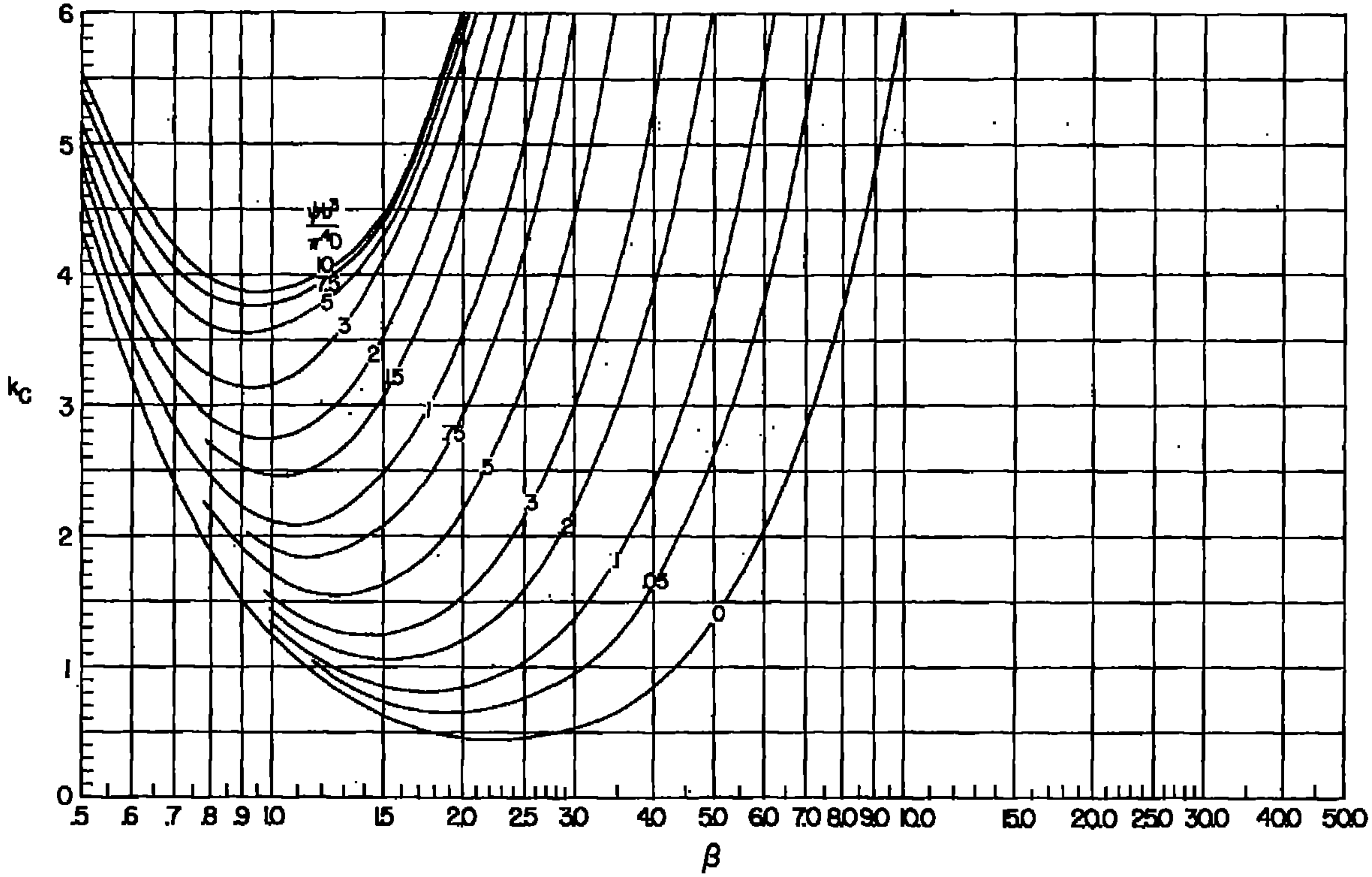

(b) $k_s = 1$.

Figure 3.- Continued.

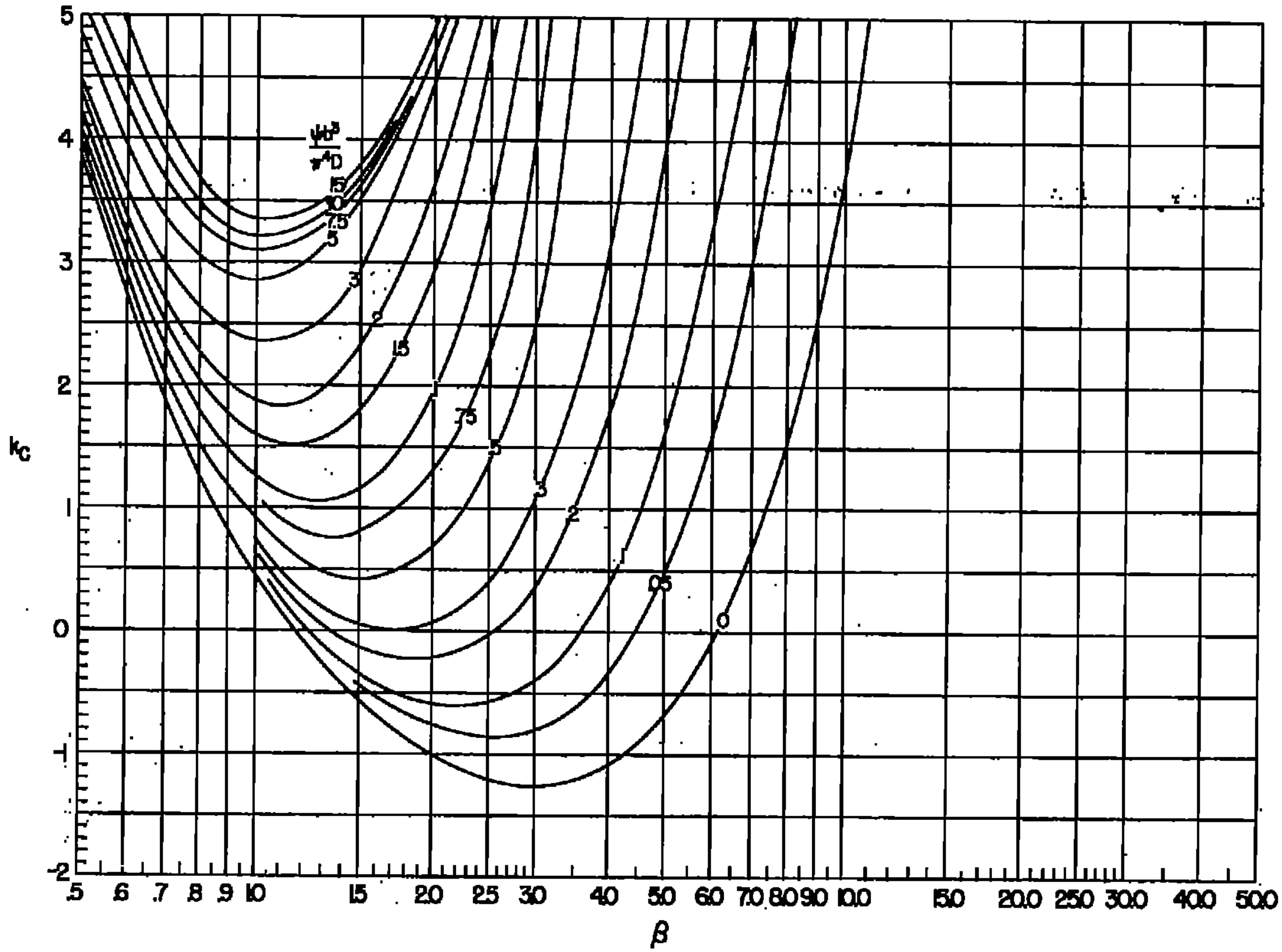

(c) $k_s = 2$.

Figure 3.- Continued.

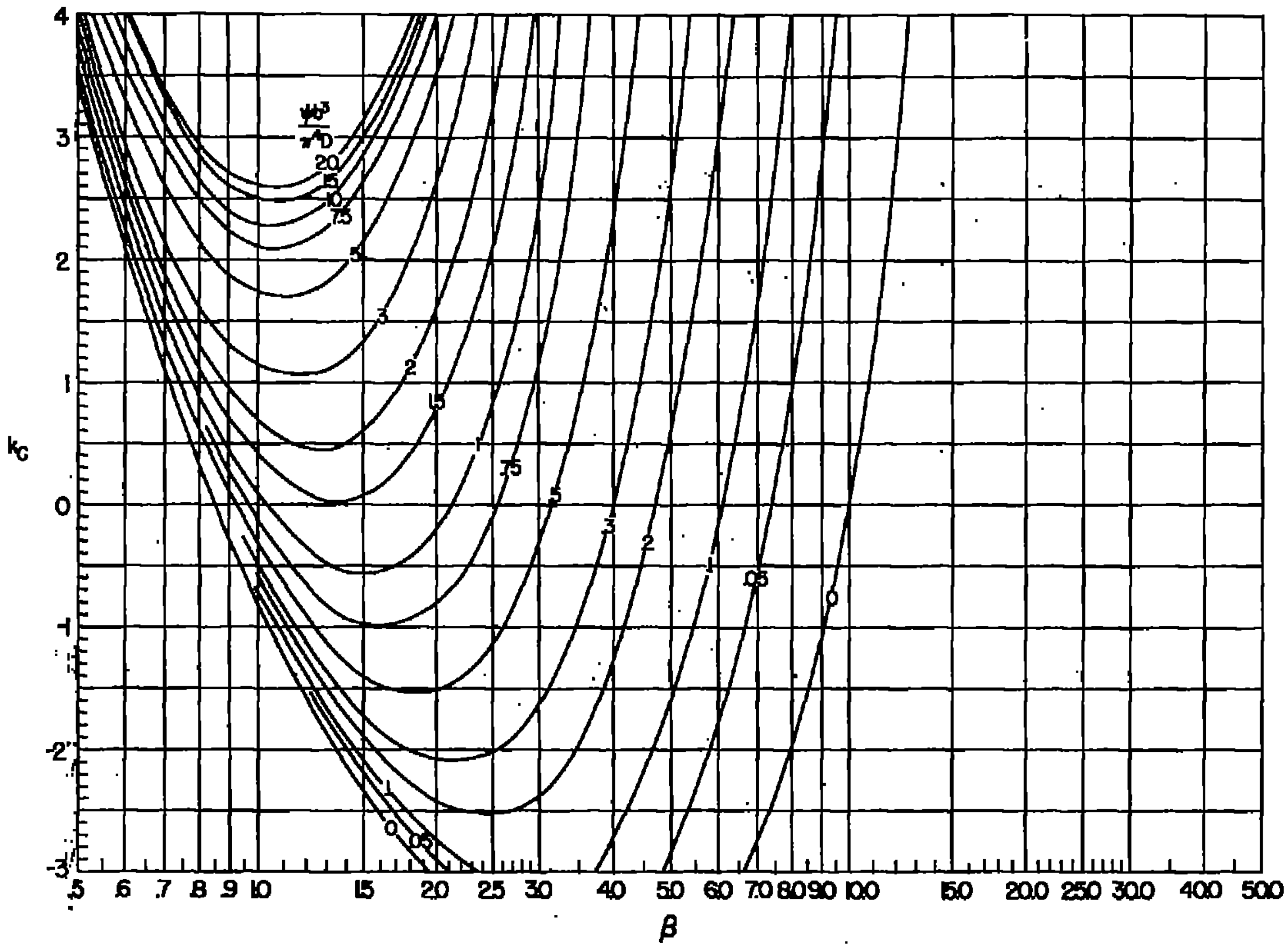

(d) $k_s = 3$.

Figure 3.- Continued.

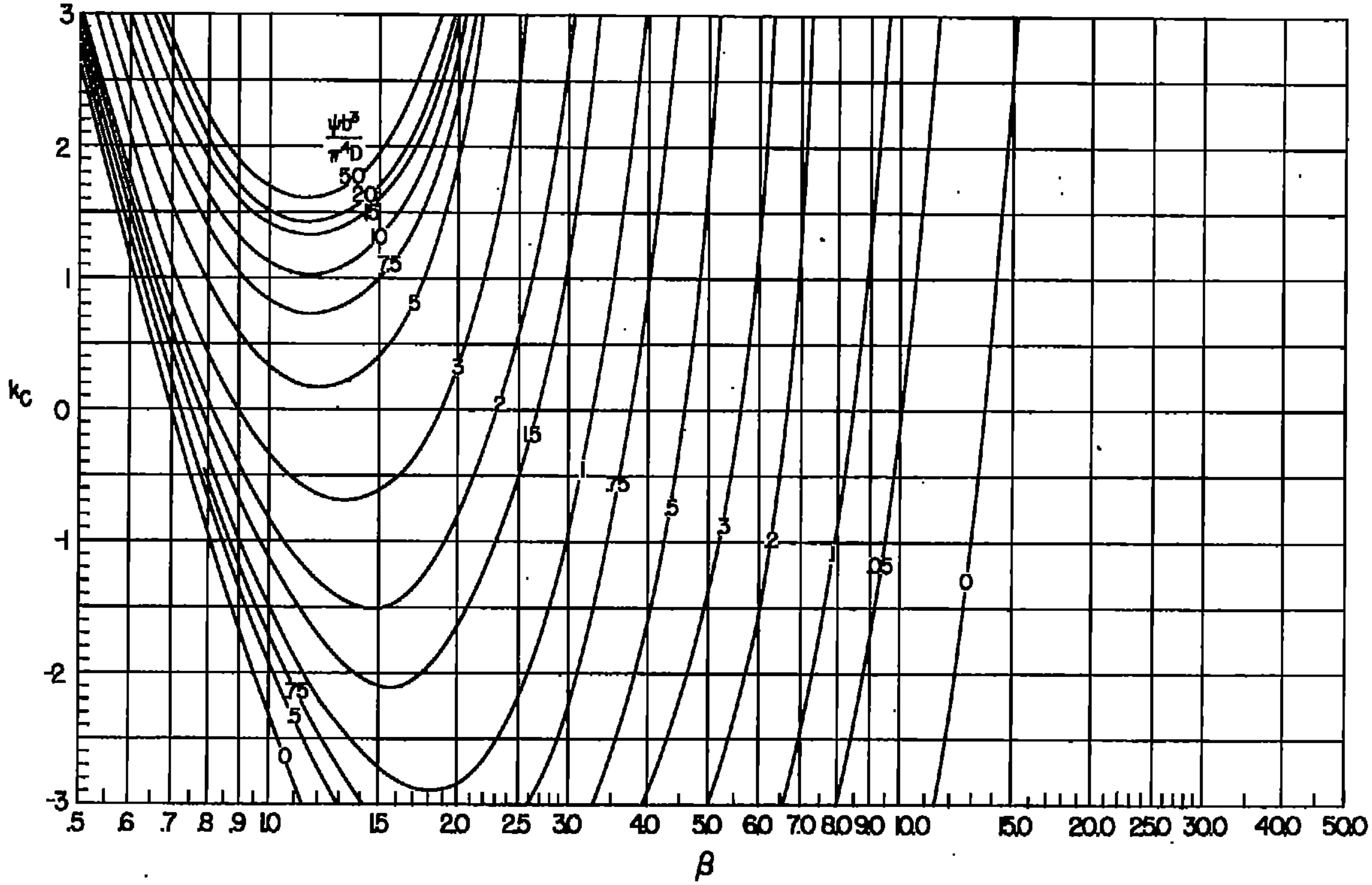

(e) $k_s = 4.$

Figure 3.- Concluded.

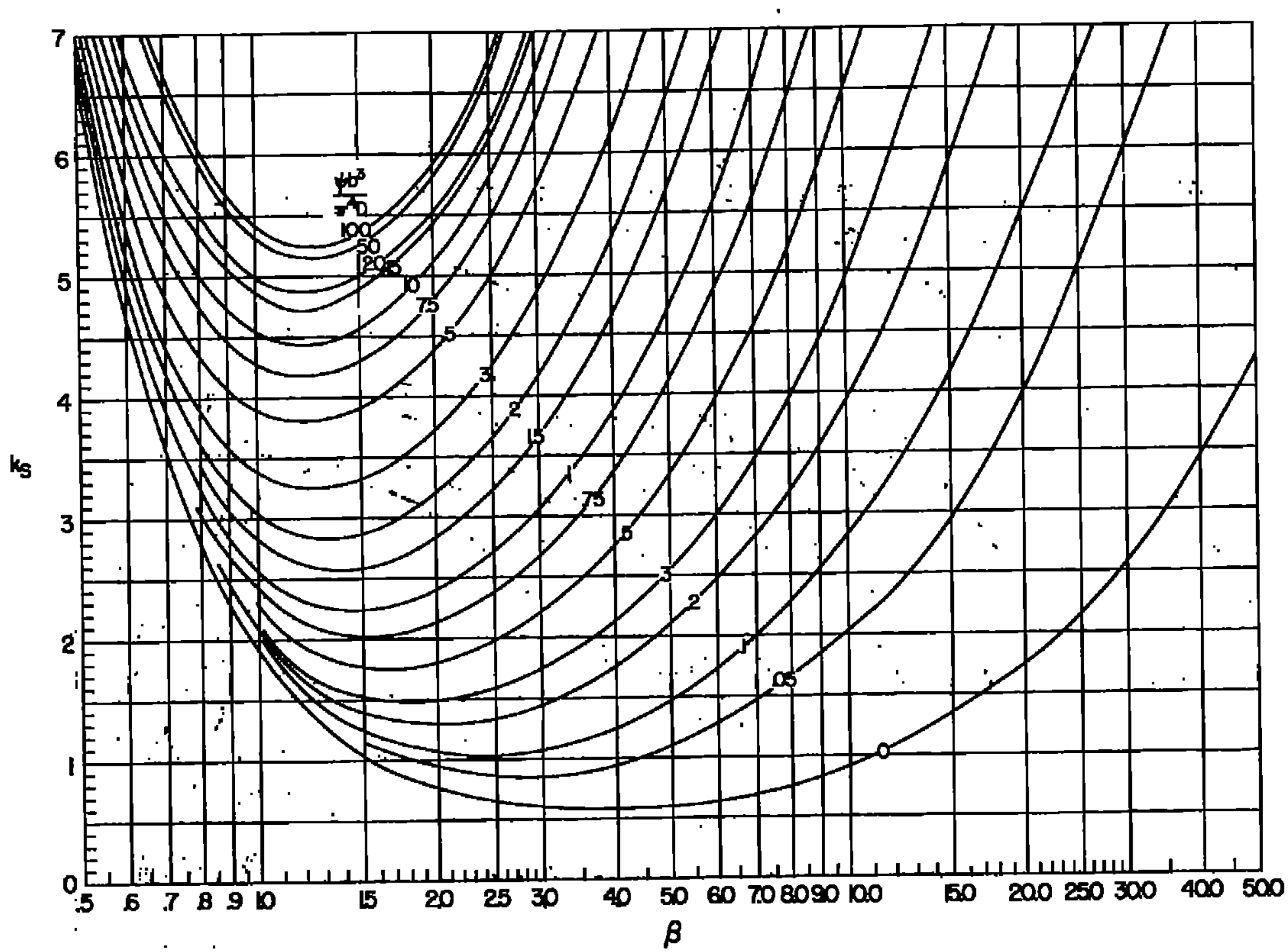

(a) $k_C = 0$.

Figure 4.- Stability curves for three-bay plate with constant compressive load.

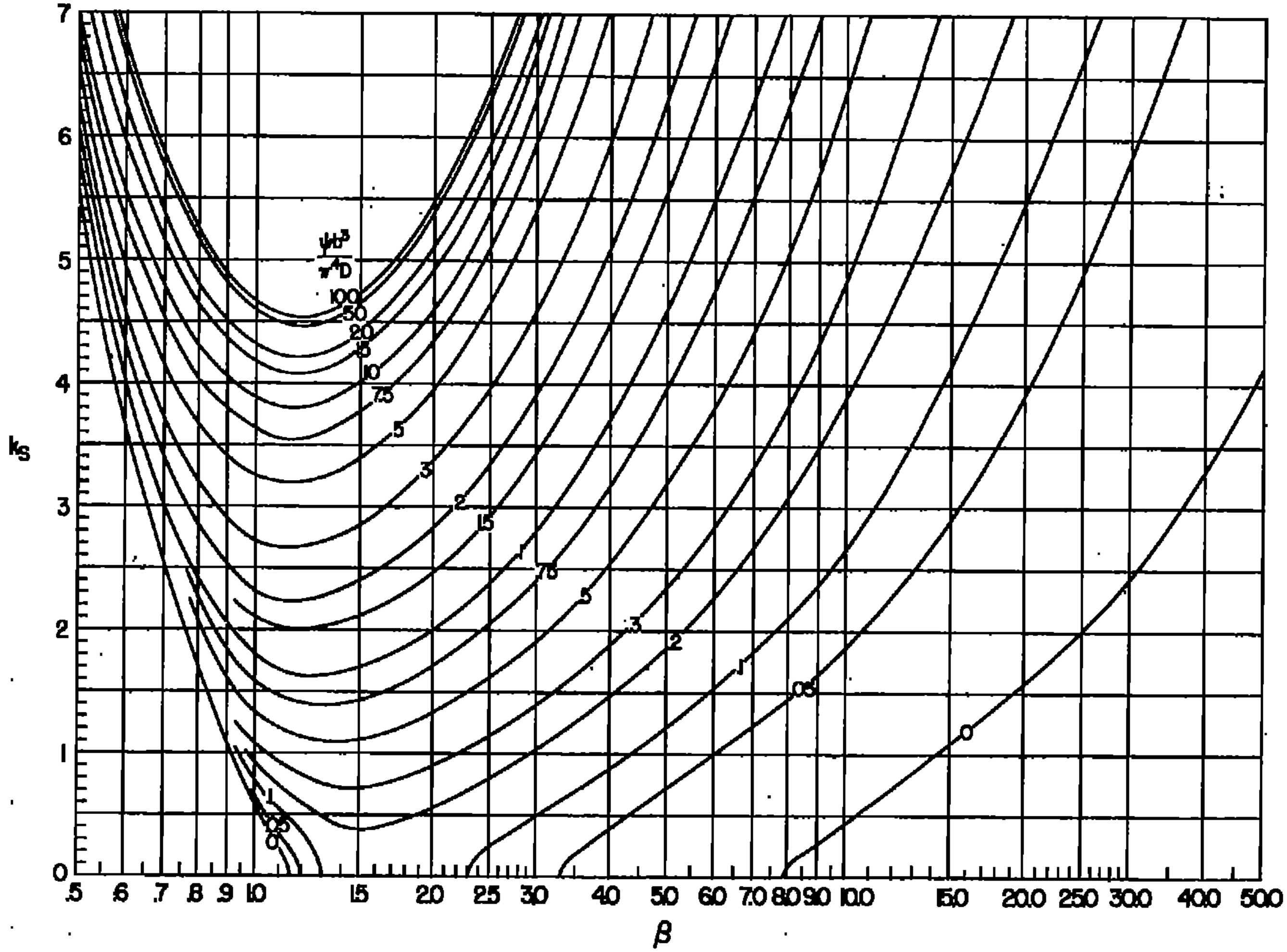

(b) $k_C = 1$.

Figure 4.- Continued.

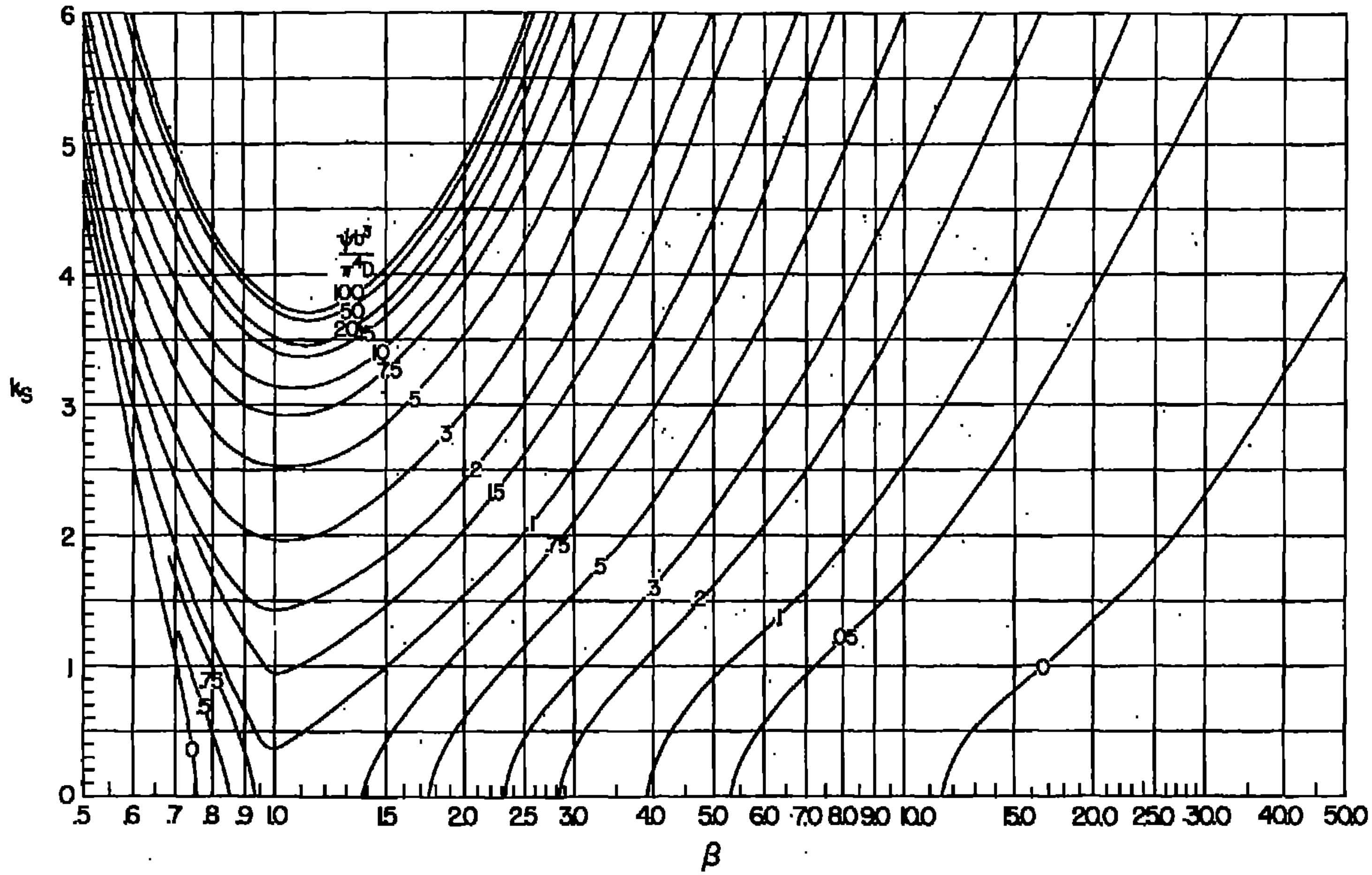

(c) $k_C = 2$.

Figure 4.- Continued.

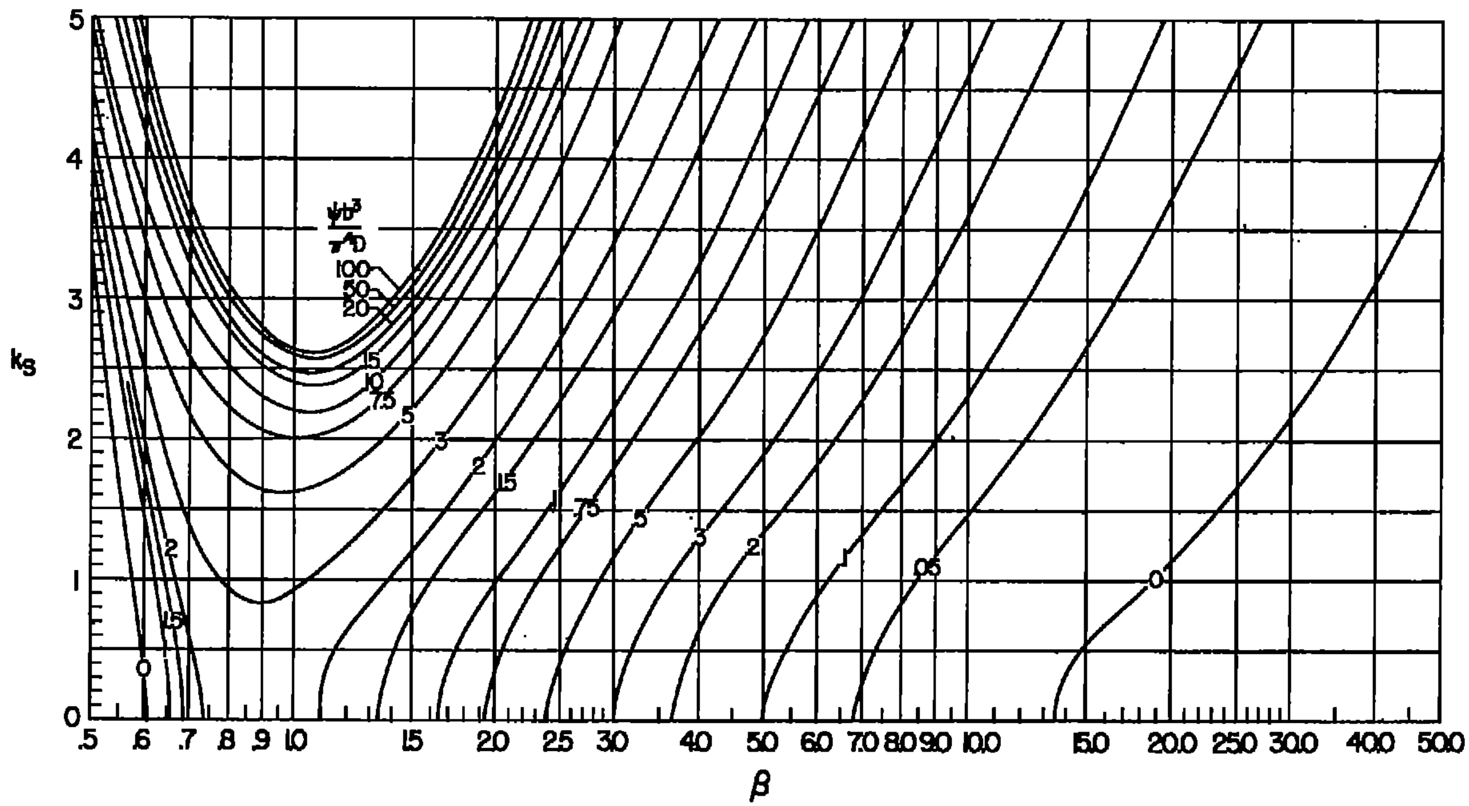

(d) $k_C = 3$.

Figure 4.- Continued.

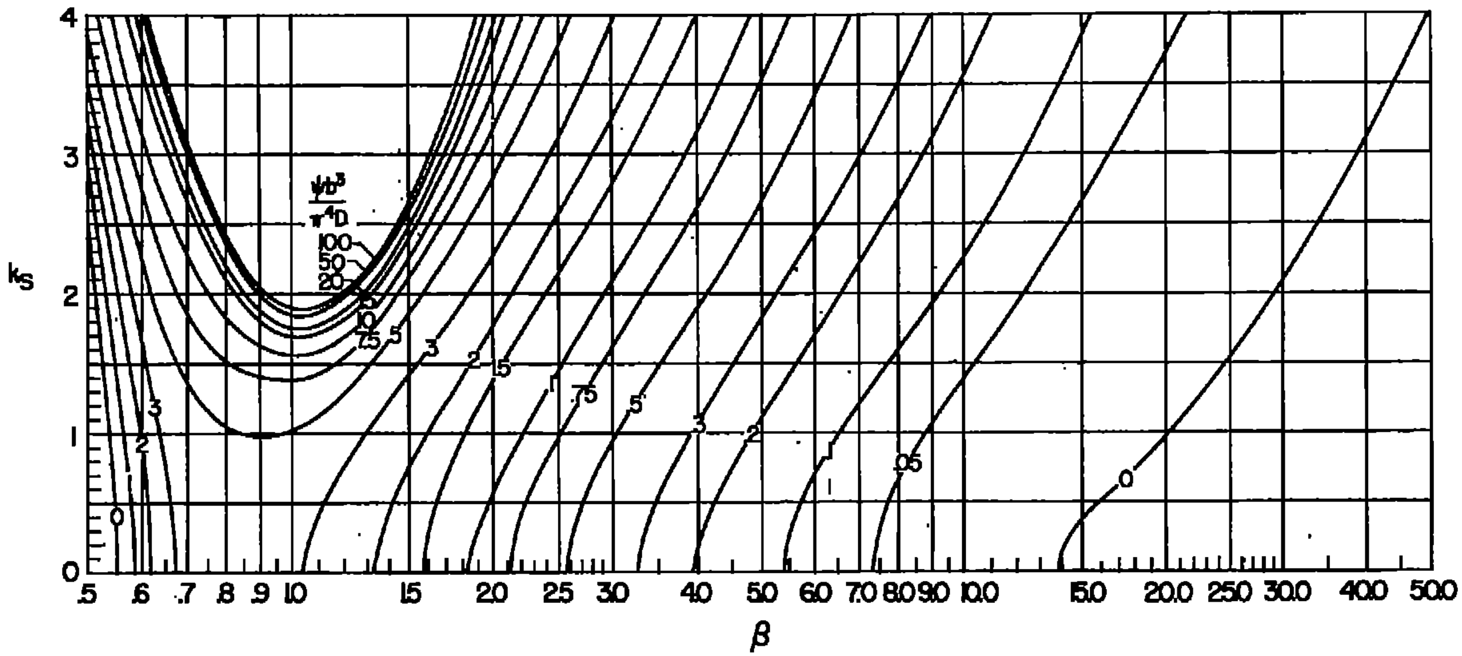

(e) $k_C = 3.5$.

Figure 4.- Concluded.

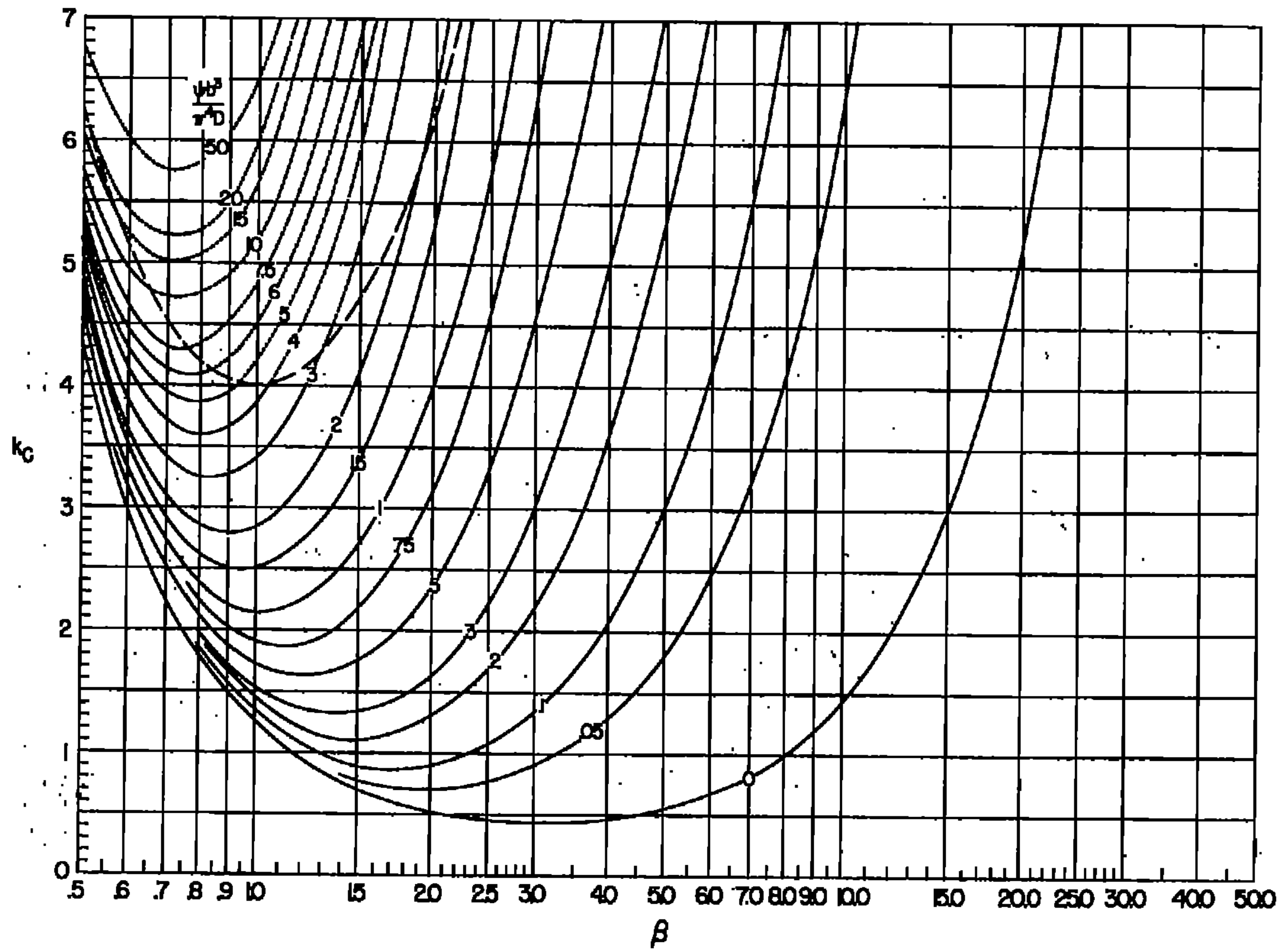

(a) $k_g = 0$. (Data are from ref. 3.)

Figure 5.- Stability curves for three-bay plate with constant shear load.

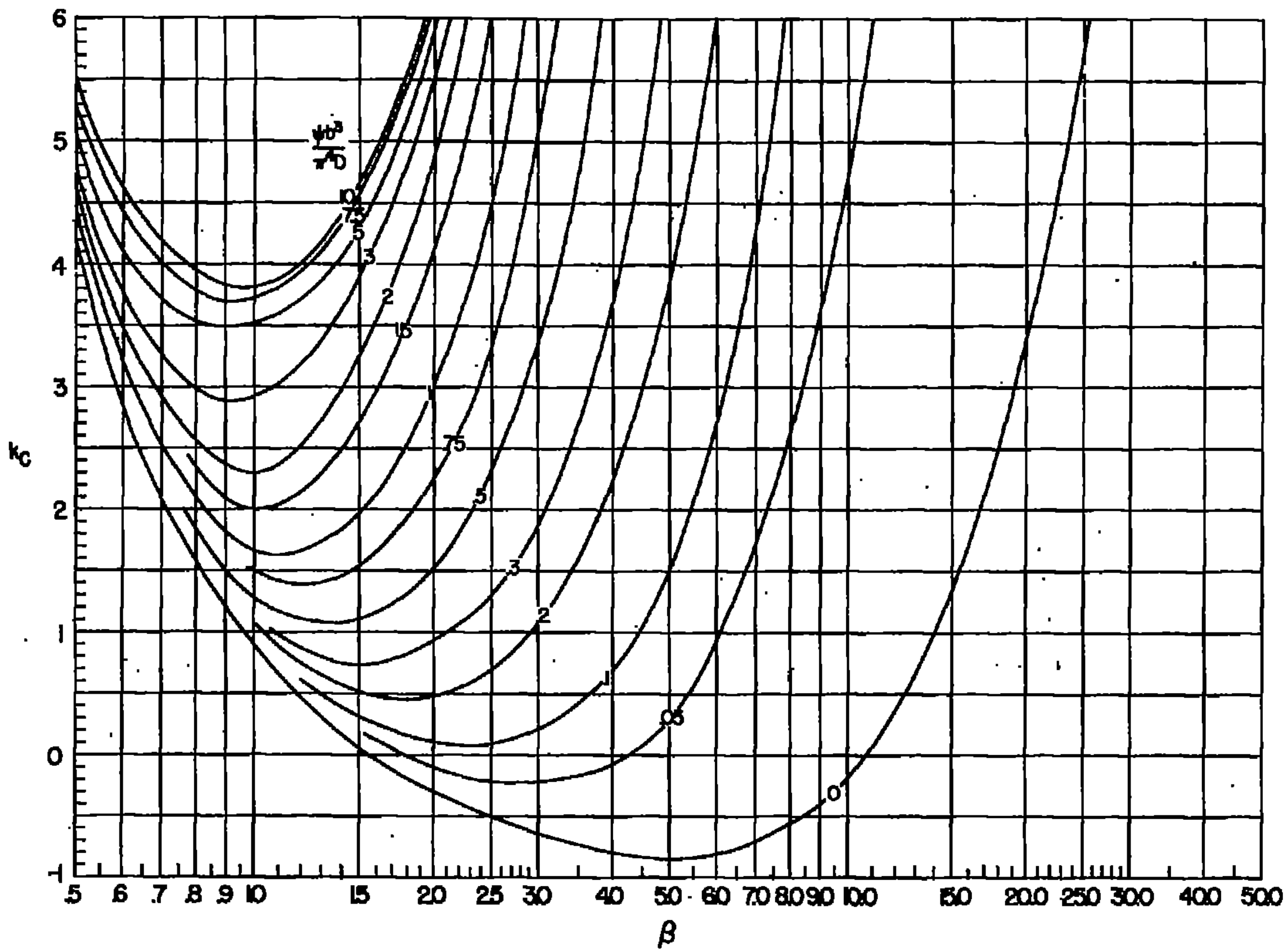

(b) $k_S = 1$.

Figure 5.- Continued.

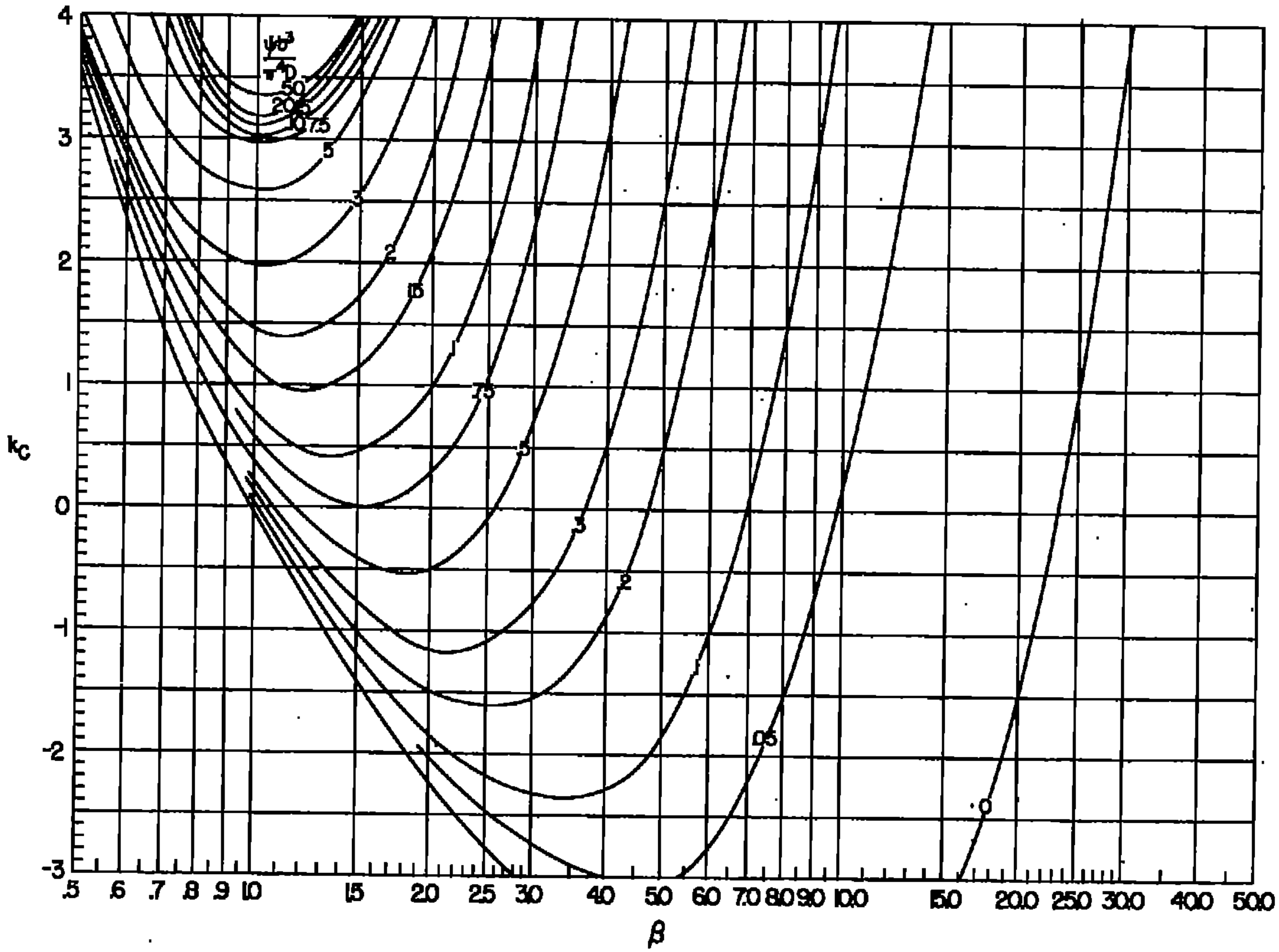

(c) $k_s = 2$.

Figure 5.- Continued.

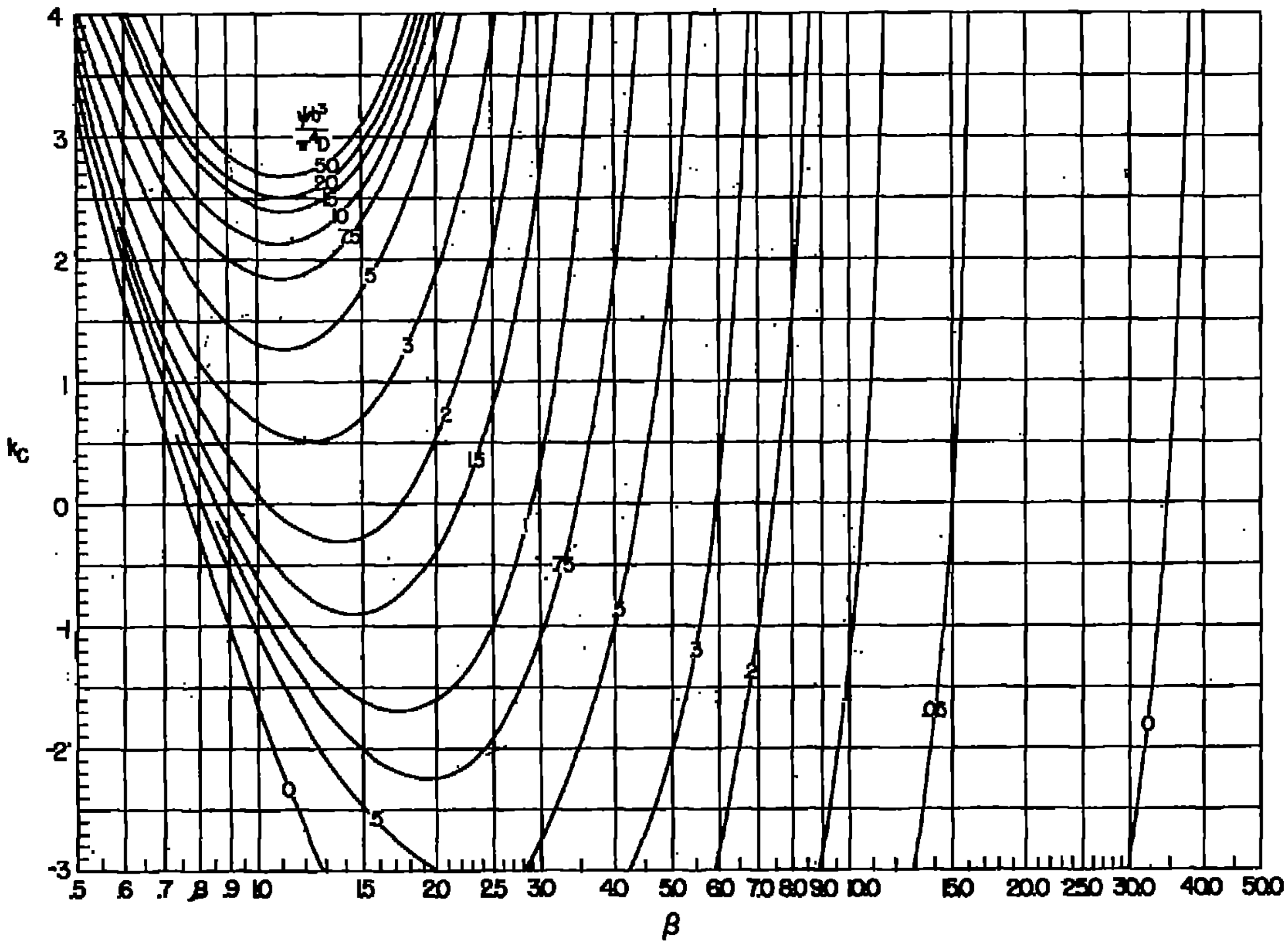

(d) $k_s = 3$.

Figure 5.- Continued.

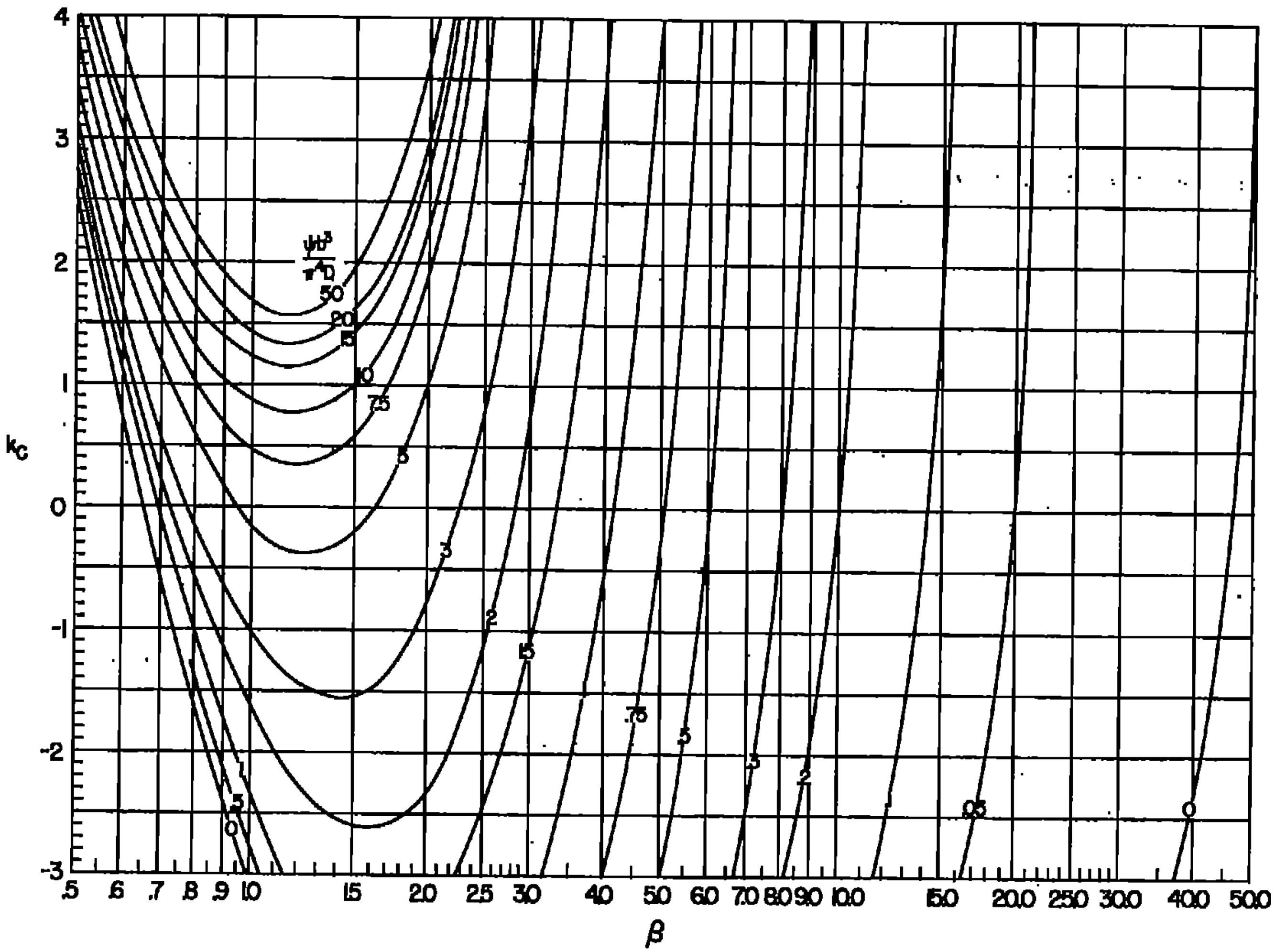

(e) $k_s = 4$.

Figure 5.- Concluded.

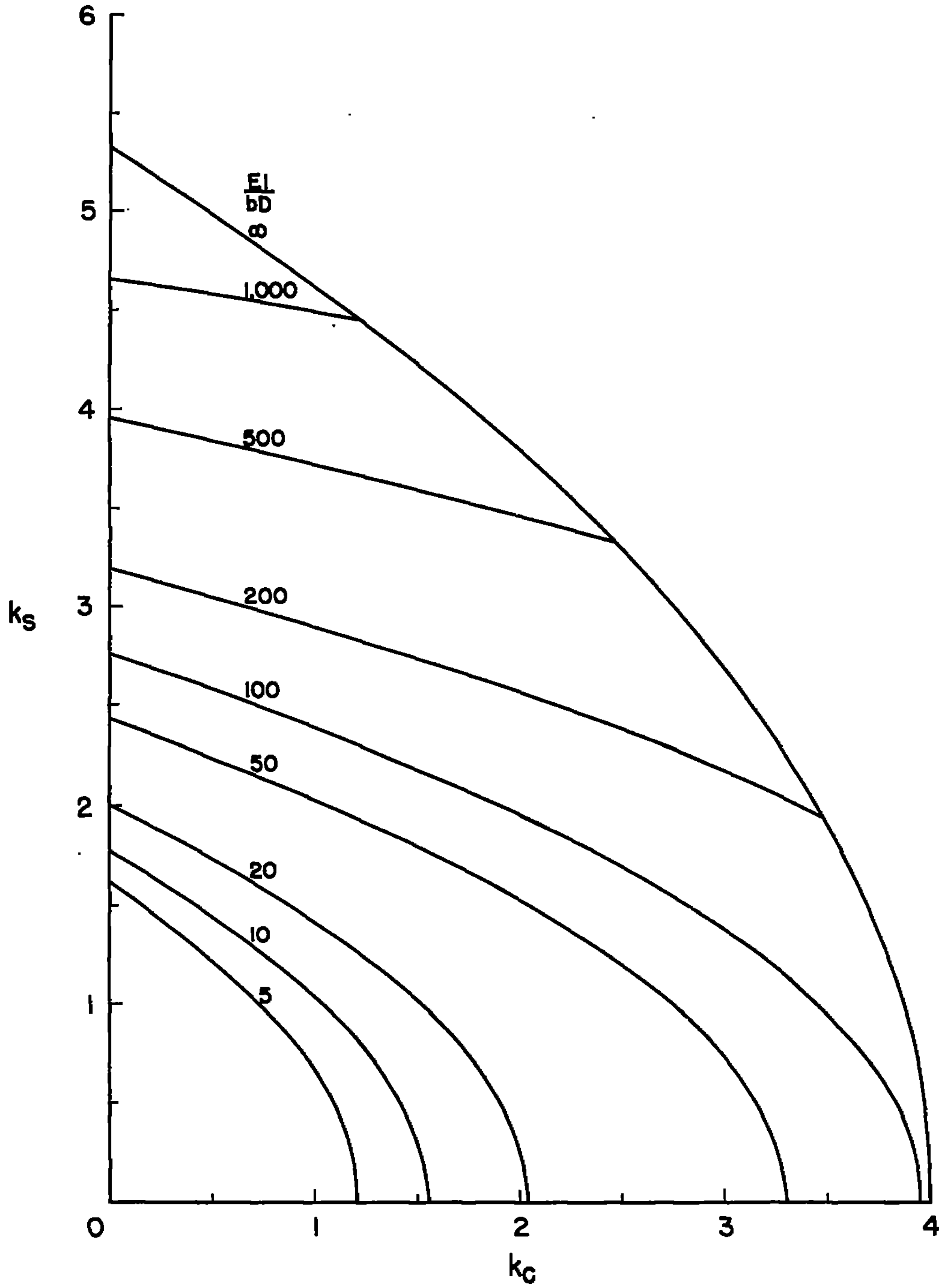

Figure 6.- Typical interaction curve for shear and compressive buckling stresses of two-bay plate. A/bt = 0.4.

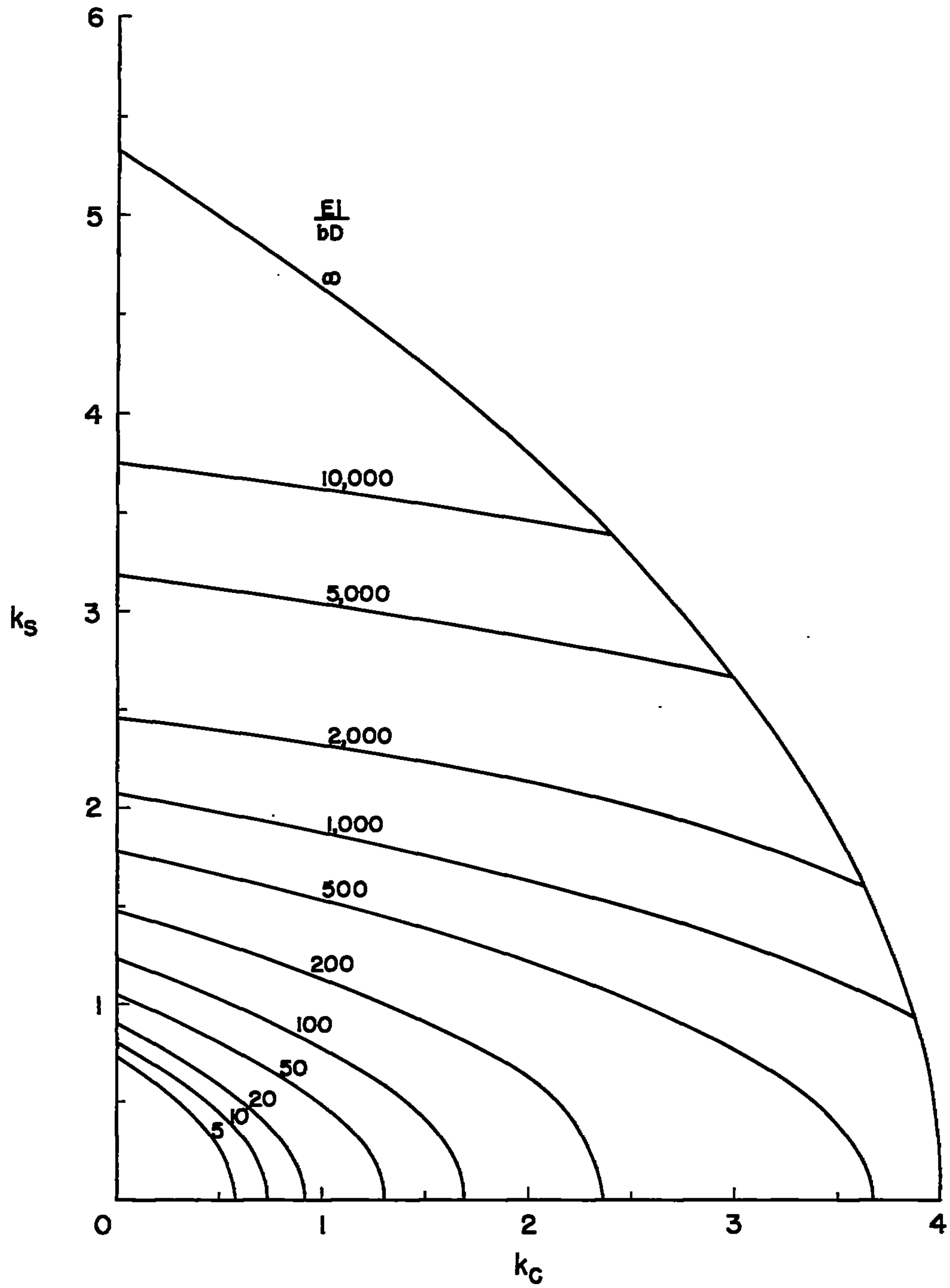

Figure 7.- Typical interaction curve for shear and compressive buckling stresses of three-bay plate. A/bt = 0.4.

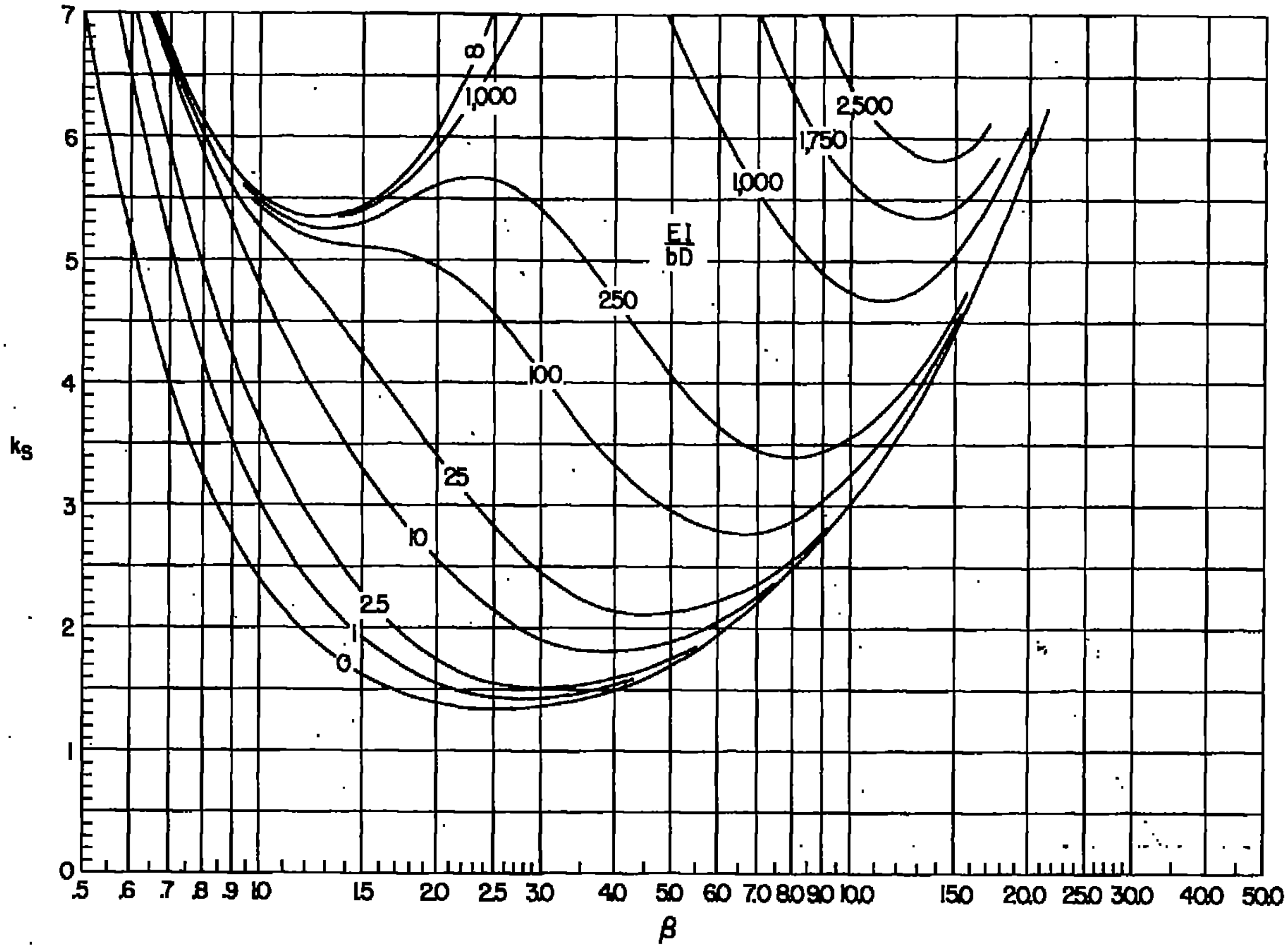

Figure 8.- Alternate form of figure 2(a).